Journal of Comparative Neurology

WILEY

JCN RESEARCH IN SYSTEMS NEUROSCIENCE THE JOURNAL OF COMPARATIVE NEUROLOGY

RESEARCH ARTICLE OPEN ACCESS

The Brain of the African Wild Dog. VI. The Motor System

Samson Chengetanai[1] | Adhil Bhagwandin[1] | Mads F. Bertelsen[2] | Therese Hård[3] | Patrick R. Hof[4,5] | Muhammad A. Spocter[1,6] | Paul R. Manger[1]

[1]School of Anatomical Sciences, Faculty of Health Sciences, University of the Witwatersrand, Johannesburg, Republic of South Africa | [2]Copenhagen Zoo, Frederiksberg, Denmark | [3]Borås Zoo, Borås, Sweden | [4]Nash Family Department of Neuroscience and Friedman Brain Institute, Icahn School of Medicine at Mount Sinai, New York City, New York, USA | [5]New York Consortium in Evolutionary Primatology, New York, New York, USA | [6]Department of Anatomy, Des Moines University, Des Moines, Iowa, USA

Correspondence: Paul R. Manger (Paul.Manger@wits.ac.za)

Received: 14 April 2025 | **Revised:** 13 June 2025 | **Accepted:** 27 June 2025

Funding: This work was supported by funding from the South African National Research Foundation (PRM), the Verizon Foundation (MAS), and the Carnegie-Wits Alumni Diaspora Program through the Carnegie Corporation of New York (MAS and PRM).

Keywords: canids | carnivores | neuroanatomy | RRID:AB_2079751 | RRID:AB_10000323 | RRID:AB_91545 | RRID:AB_10000343 | RRID:AB_10000340 | RRID:AB_10000321 | RRID:AB_2187552 | RRID:AB_509997 | RRID:AB_11204707 | RRID:AB_2088494

ABSTRACT

Social behaviors in the African wild dog involve a range of complex movements, including biting, pushing, embracing, mounting, face and muzzle licking, paw placement, play fighting, and wrestling. In this study, we employ a range of architectural and immunohistochemical stains to provide a qualitative description of the motor system in the brain of one representative individual of the African wild dog. The appearance of the motor system in the African wild dog does not differ substantively to that reported in other carnivores and is neurochemically like that of the domestic dog; however, one significant difference was detected: the presence of a distinct fascicle of protoplasmic commissural dendrites at the rostral pole of the hypoglossal nucleus. The chemoarchitecture and complement of motor cortical areas and dorsal thalamus, striatopallidal complex and associated nuclei, cerebellum, red nucleus, descending motor pathways, inferior olivary nuclear

Abbreviations: 10n, root of vagus nerve; 12n, root of hypoglossal nerve; 17, Brodmann area 17, primary visual cortex; 18, Brodmann area 18, secondary visual cortex; 19, Brodmann area 19, tertiary visual cortex; 21, Brodmann area 21, visual cortex; 3a, proprioceptive somatosensory cortical area; 3n, root of oculomotor nerve; 7Sp, ventral horn, laminae 7 of Rexed.; 8Sp, ventral horn, laminae 8 of Rexed.; 9Sp, ventral horn, laminae 9 of Rexed.; A10, ventral tegmental area; A8, retrorubral nucleus; A9l, substantia nigra, lateral; A9m, substantia nigra, medial; A9pc, substantia nigra, pars compacta; A9v, substantia nigra, ventral; AAF, anterior auditory field; AcbC, accumbens nucleus, core; AcbSh, accumbens nucleus, shell; AD, anterodorsal thalamic nucleus; AHC, anterior hippocampal continuation; AI, primary auditory cortex; AII, secondary auditory cortex; AM, anteromedial thalamic nucleus; Amb, nucleus ambiguus; AON, anterior olfactory nucleus; AP, area postrema; AV, anteroventral thalamic nucleus; C, caudate nucleus; CB, calbindin; CC, central canal of spinal cord; CeCV, central cervical nucleus of the spinal cord; ChAT, choline acetyltransferase; CL, centrolateral thalamic nucleus; Cl, claustrum; cp, cerebral peduncle; CR, calretinin; cu, cuneate fasciculus; Cu, cuneate nucleus; CuR, rotundus part of cuneate nucleus; ECu, external cuneate nucleus; EGP, external globus pallidus; GCL, granule cell layer of cerebellar cortex; GiCRt, gigantocellular reticular nucleus; gr, gracile fasciculus; Gr, gracile nucleus; ic, internal capsule; icp, inferior cerebellar peduncle; IG, induseum griseum; IGP, internal globus pallidus; III, oculomotor nucleus; IOD, inferior olive, dorsal nucleus; IOM, inferior olive, medial nucleus; IOPr, inferior olive, principal nucleus; IP, interpeduncular nucleus; lcs, lateral corticospinal tract; lf, lateral funiculus; lfp, longitudinal fasciculus of the pons; ll, lateral lemniscus; lot, lateral olfactory tract; LRt, lateral reticular nucleus; M1, primary motor cortex (Brodmann area 4); m5, motor root of the trigeminal nerve; mcp, middle cerebellar peduncle; MD, mediodorsal thalamic nucleus; ml, medial lemniscus; ML, molecular layer of cerebellar cortex; mlf, medial longitudinal fasciculus; mmt, mammillothalamic tract; MOB, main olfactory bulb; NeuN, neuronal nuclear marker; NFH, neurofilament H; NI, interpositus cerebellar nucleus; NL, lateral cerebellar nucleus; NM, medial cerebellar nucleus; NSP, nigrostriatal projection; OT, optic tract; OV, olfactory ventricle; P, putamen; Pc, paracentral thalamic nucleus; pcd, protoplasmic commissural dendrites; PCL, Purkinje cell layer of cerebellar cortex; PCRt, parvocellular reticular nucleus; PIR, piriform cortex; Pn, pontine nucleus; PnO, pontine reticular nucleus, oral part; PP, posterior parietal visual areas; PreM, premotor cortical area (Brodmann area 6); Pv, parietal-ventral somatosensory cortical area; PV, parvalbumin; pVII, preganglionic motor neurons of the superior salivatory nucleus or facial nerve; py, pyramidal tract; pyx, decussation of the pyramidal tract; RMC, red nucleus, magnocellular part; RPC, red nucleus, parvicellular part; RtTg, reticulotegmental nucleus of the pons; RtTgP, reticulotegmental nucleus of the pons, pericentral part; s5, sensory root of trigeminal nerve; SI, primary somatosensory cortical area; SII, second somatosensory cortical area; SIII, third somatosensory cortical area; SMA, supplementary motor cortical area; SNR, substantia nigra, reticular part; Sol, solitary nuclear complex; sol, solitary tract; sp5, spinal trigeminal tract; Sp5C, spinal trigeminal nucleus, caudal part; SS, suprasylvian visual areas; STh, subthalamic nucleus; T, temporal visual region; TH, tyrosine hydroxylase; TTd, dorsal taenia tecta; tth, trigeminothalamic tract; Tu, olfactory tubercle; VA, ventral anterior thalamic nucleus; VC, ventral cochlear nuclear complex; vf, ventral funiculus; vGlut2, vesicular glutamate transporter 2; VIId, facial nerve nucleus, dorsal part; VIIv, facial nerve nucleus, ventral part; VL, ventrolateral thalamic nucleus; VM, ventromedial thalamic nucleus; Vmot, motor division of trigeminal nerve nucleus; VP, ventral posterior thalamic nuclear complex; X, dorsal motor vagus nucleus; XI, accessory nerve nucleus; XII, hypoglossal nucleus; XIIdl, hypoglossal nucleus, dorsolateral part; XIIm, hypoglossal nucleus, medial part; XIIvl, hypoglossal nucleus, ventrolateral part; ZI, zona incerta.

Associate Editor: Jorge Mpodozis.

complex, cranial nerve motor nuclei, and ventral horn of the cervical spinal cord of the African wild dog do not reveal qualitative differences to that observed in the domestic dog. At the rostral pole of the hypoglossal nucleus, protoplasmic commissural dendrites form a distinct fascicle, this fascicle being a feature that has not been reported in other mammals. The presence of this feature indicates complex neural control of the tongue and may facilitate vocalization control through the potential combination of lateralized aspects of vocalizations in a nucleus playing a major role in the production of vocalizations.

1 | Introduction

The mammalian motor system is composed of multiple cortical areas, fiber tracts, and nuclear complexes. Structures forming the motor system include the motor areas of the cerebral cortex, the motor nuclei of the dorsal thalamus, the striatopallidal complex and associated nuclei, cerebellum, red nucleus, the descending motor pathways including the pyramidal tract, the inferior olivary nuclear complex, the cranial nerve motor nuclei, and the ventral horn of the cervical spinal cord (e.g., Møller 2006). While involved in the production and fine control of cognitive-based voluntary actions (e.g., Prevosto and Sommer 2013), certain parts of the motor system also assimilate affective context into the generated movements (e.g., Floresco 2015).

The African wild dog is a highly social canid species (Van den Berghe et al. 2019; Creel and Creel 2002; Walker et al. 2017), but our systematic studies of the sensory systems of the brain of the African wild dog to date have not revealed any overt specializations that may support wild dog sociality (Chengetanai et al. 2020a, Chengetanai et al. 2020d, Chengetanai et al. 2025). Movement is an integral part of the social interactions of the African wild dog, with actions such as biting, assaults, mounting, licking, head placement, body rubbing, play fighting, fighting,

TABLE 1 | Sources and dilution of antibodies used in the current study.

Antibody	Host	Immunogen	Manufacturer	Catalogue No.	Reference	Dilution	RRID
NeuN	Rabbit	GST-tagged recombinant protein corresponding to mouse NeuN	Merck-Millipore	ABN78C3	Ngwenya et al. 2016	1:500	AB_11204707
ChAT	Goat	Human placental enzyme	Merck-Millipore	AB144P	Laux et al. 2012; Kaiser et al. 2011	1:3000	AB_2079751
TH	Rabbit	Purified tyrosine hydroxylase from rat adrenal	Merck-Millipore	AB151	Piskuric et al. 2011	1:3000	AB_10000323
PV	Rabbit	Rat muscle parvalbumin	Swant	PV28	Celio 1990	1:10000	AB_10000343
CB	Rabbit	Rat recombinant calbindin D-28k	Swant	CB38a	Celio 1990	1:10000	AB_10000340
CR	Rabbit	Recombinant human calretinin containing a 6-his tag at the N-terminal	Swant	7699/3H	Schwaller et al. 1997	1:10000	AB_10000321
vGlut2	Mouse	Recombinant protein from rat vGlut2	Merck-Millipore	MAB5504	Wong et al. 2008; Griffin et al. 2010	1:4000	AB_2187552
SMI-32	Mouse	Non-phosphorylated epitope of neurofilament H from rat hypothalami	Covance	SMI-32R	Sternberger and Sternberger 1983	1:1000	AB_509997

Abbreviations: CB = calbindin; ChAT = choline acetyltransferase; CR = calretinin; NeuN = neuronal nuclear marker; PV = parvalbumin; SMI-32 = neurofilament H; TH = tyrosine hydroxylase; vGlut2 = vesicular glutamate transporter 2.

wrestling, and vocalizations, being integral actions used in the social life of this species (Walker et al. 2017; Van den Berghe et al. 2019). Given the assimilation of affect into movement and the importance of affect in sociality for dogs (e.g., Väätäjä et al. 2021), there is potential for the motor system of the African wild dog to have developed specializations. It is also important to note that the forelimb of the African wild dog has undergone several anatomical modifications for long-distance running related to their exhaustive predation strategy that may increase stride length, running speed, and stability compared to other canids (H. F. Smith et al. 2020), indicating the potential for specializations of the motor system to accommodate these adaptive anatomical reconfigurations.

While studies of the motor cortex (Woolsey 1933; W. K. Smith 1935; Górska 1974; Hof et al. 1996), motor thalamus (e.g., Sakai et al. 1983), and other aspects of the motor system in the domestic dog (e.g., Singer 1962; Dattam et al. 2012) are available, studies of the motor system in non-domestic canids and their close relatives are infrequent (e.g., Buxton and Goodman 1967; Foster et al. 2024). In this study, we extend our detailed, systems-level, analysis of the African wild dog brain (Chengetanai et al. 2020a-Chengetanai et al. 2020d, Chengetanai et al. 2025) by providing a qualitative description of the motor system found in the brain of the African wild dog.

2 | Materials and Methods

2.1 | Specimens

Ten adult African wild dog brains were obtained from Borås Zoo, Sweden (see Chengetanai et al. 2020a for full details of animals, permits, and collection and treatment of tissue). Antemortem observations for all these animals revealed that they were in good health with no obvious neural deficits or behavioral abnormalities and were euthanized for population management reasons (Bertelsen 2018). While these animals were bred in captivity, they were housed in a large naturalistic enclosure in a sizeable pack and exhibited all normal social behaviors. All animals were treated and used according to the guidelines of the University of the Witwatersrand Animal Ethics Committee (AESC No. 2012/53/01), which parallel those of the National Institutes of Health (NIH) for the care and use of animals in scientific experimentation. In the current study, the whole brain of one of these specimens (LP2, a male with a brain mass of 141.5 g) was sectioned, stained, and analyzed. While this study is primarily based on our observations from a single specimen, in a previous study this specimen and five others underwent magnetic resonance (MR) imaging (Chengetanai et al. 2020a). When comparing the specimen used herein to these other MR scanned brains, no differences in terms of overall morphology of the motor system, at the level of MRI resolution, were noted. We thus assumed that this specimen is representative of the species but acknowledge that the use of a single specimen may introduce errors into the interpretation made and thus temper our observations and conclusions accordingly.

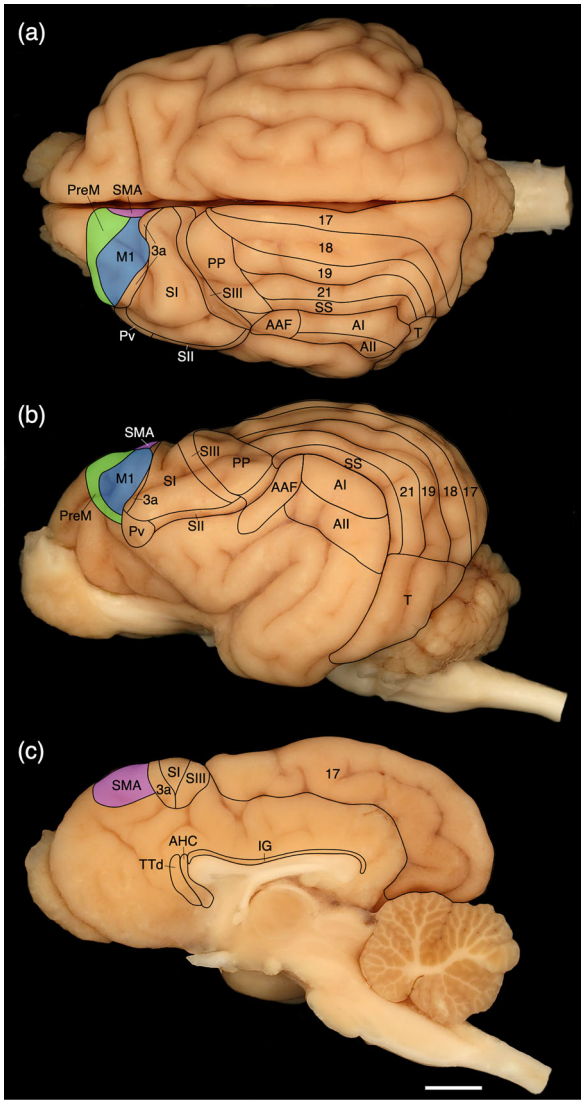

FIGURE 1 | (a) Dorsal, (b) lateral, and (c) mid-sagittal views of the African wild dog brain showing the approximate location of the motor cortical areas determined with architectural and immunohistochemical stains in the current study (see Figure 2). Within the motor cortical territory of the African wild dog, we identified three areas, including the primary motor cortex (M1, Brodmann area 4, blue shading), the PreMotor area (PreM, Brodmann area 6, green shading), and the supplementary motor area (SMA, purple shading). These are depicted in relation to cortical areas involved in olfaction (Chengetanai et al. 2020b), audition (Chengetanai et al. 2020c), vision (Chengetanai et al. 2020d), and somatosensation (Chengetanai et al. 2025). Scale bar in (c) = 1 cm and applies to all. See the list for abbreviations.

2.2 | Sectioning, Immunohistochemical Staining, Antibody Characterization, and Specificity

Prior to sectioning, the brain was allowed to equilibrate in 30% sucrose in 0.1 M PB at 4°C then frozen in crushed dry ice and sectioned into 50-μm-thick coronal sections on a freezing microtome into a 1 in 20 series of sections. Consecutive series of sections were stained for Nissl, myelin, and immunolabeled for neuronal nuclear marker (NeuN), choline acetyltransferase (ChAT), tyrosine hydroxylase (TH), parvalbumin (PV), calbindin (CB), calretinin (CR), neurofilament H (NFH), and vesicular glutamate transporter 2 (vGlut2). The remaining 10 series of

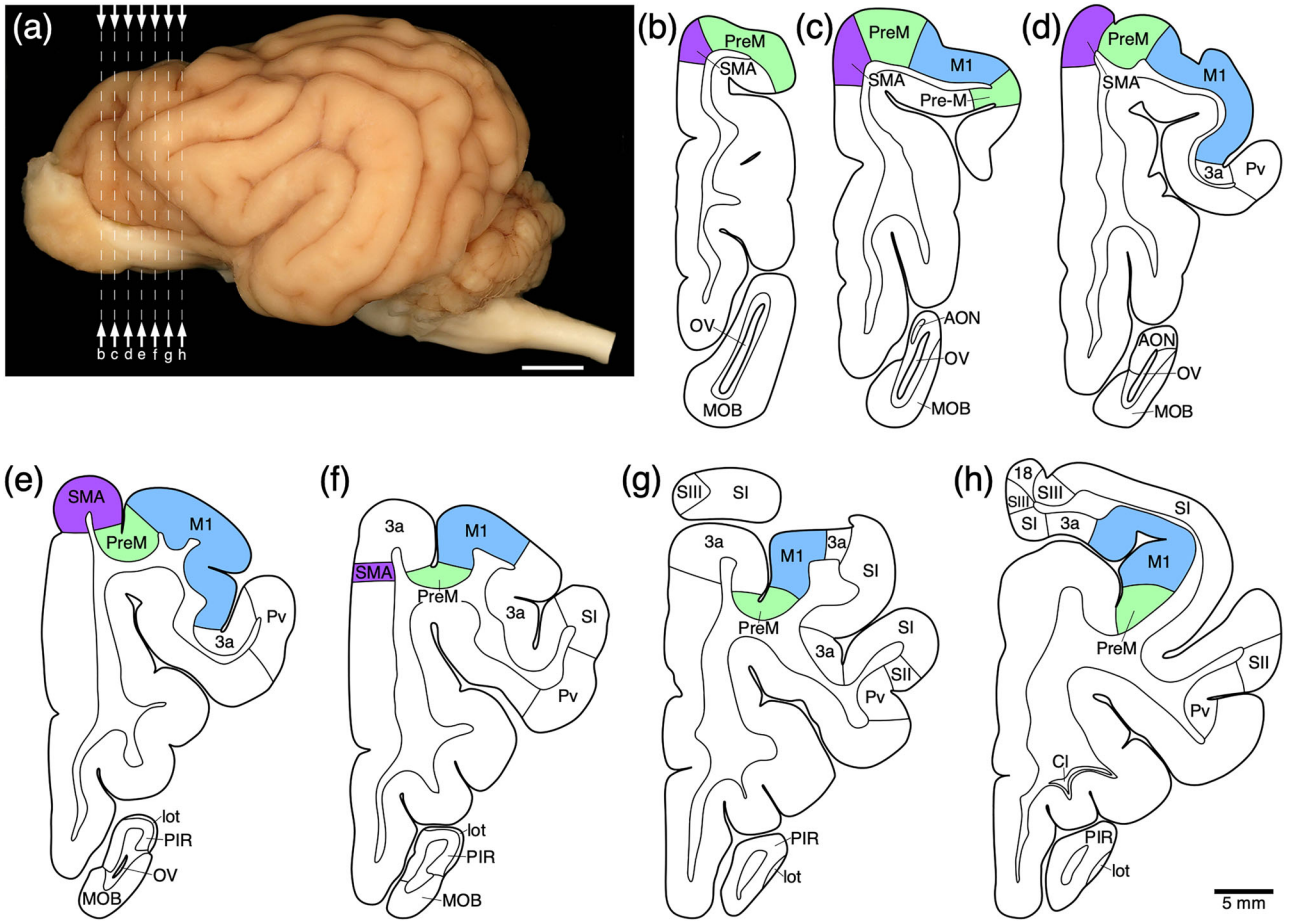

FIGURE 2 | Diagrammatic reconstructions of coronal sections through the African wild dog brain delineating the identified motor cortical areas and certain other sub-cortical structures. In all diagrams, dorsal is to the top and medial to the left. A lateral view of the African wild dog brain with the approximate level of the reconstructed sections is shown in (a). The most rostral section drawn is shown in (b), while the most caudal section is shown in (h). Each diagram is ~2000 μm apart. The various cortical areas are represented with differing colors. See the list for abbreviations.

sections were stored in an antifreeze medium for future use. The sections used for Nissl staining were mounted on 0.5% gelatine coated glass slides, allowed to dry for 48 h, cleared in a solution of 1:1 chloroform and 100% alcohol overnight. The sections were then hydrated in a graded series of alcohol (100%, 100%, 95%, 70%, and 50%), after which the sections were stained with 1% cresyl violet (Sigma-Aldrich, C5042, PubChem CID: 135445693). The sections were then washed in distilled water; excess cresyl violet stain removed in 50% alcohol; differentiated in 70% alcohol with some added acetic acid; dehydrated in 95%, 100%, and 100% alcohol; cleared in xylene; and cover-slipped with Depex. The sections used for myelin staining were refrigerated for 2 weeks in 5% formalin then mounted on 1.0% gelatine-coated slides and stained with a modified silver stain (Gallyas 1979). Full details of the immunostaining protocol, and the characterization and specificity of the antibodies used in the current study are provided in an earlier publication (Chengetanai et al. 2020b) and are not repeated here (see Table 1 for a synopsis of antibody characterization and use in the current study).

2.3 | Analysis

In this study, we provide a qualitative description of the architecture of the motor system in the brain of an African wild dog (LP2). While broadly guided by previous studies in the domestic dog (Singer 1962), we systematically examined all coronal sections of all stains at low magnification throughout the brain of LP2 to identify regions of interest that correlated with previous reports on the structure of the motor system. For example, when specific motor nuclei were identified, we examined the sections in which these nuclei were identified at a range of magnifications to determine precise borders and to note how different nuclei forming this region of the brain were differentiated from each other to develop the description provided. As a second example, the primary motor cortical area (M1/area 4) was readily delineated due to the layer 5 gigantopyramidal (or Betz) neurons, as well as the absence of a layer 4. Camera-lucida drawings (see Section 3.1) were made of the right hemisphere and the borders of M1 marked. The cortical territories surrounding M1 were then examined in detail, using all stains, to determine the additional motor areas surrounding M1 and delineate them on the camera-lucida drawings. These drawings were aligned with images of the brain to determine the location of these cortical areas on the cortical mantle and the boundaries drawn. Our analysis is primarily compared to the atlas of the dog brain provided by Singer (1962) although we employ, as much as is reasonable, the nomenclature provided by Jones (2007) and Paxinos et al. (2009).

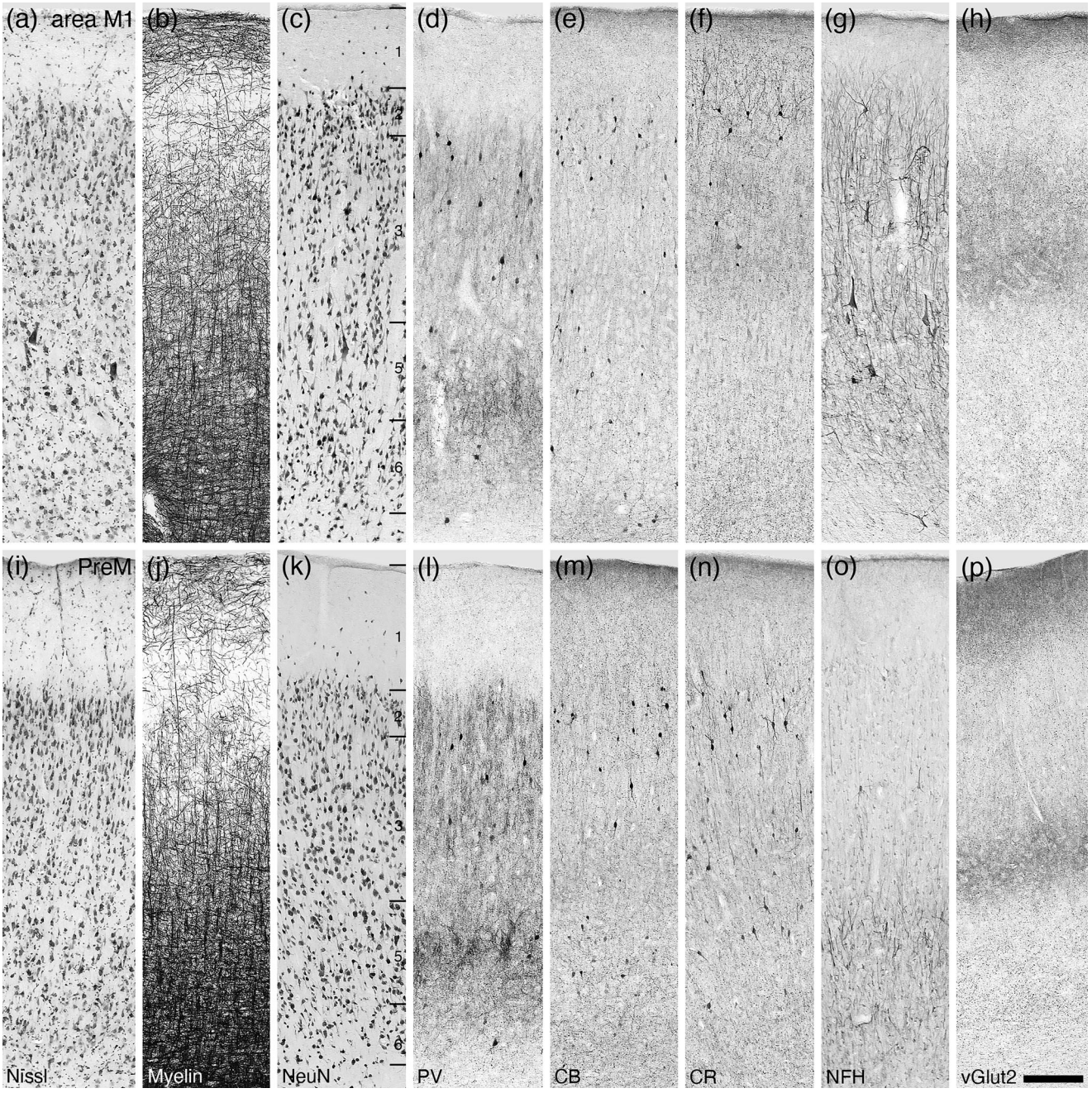

FIGURE 3 | Photomicrographs of Nissl (a, i), myelin (b, j), neuronal nuclear marker (NeuN) (c, k), parvalbumin (PV) (d, l), calbindin (CB) (e, m), calretinin (CR) (f, n), neurofilament H (NFH) (g, o), and vesicular glutamate transporter 2 (vGlut2) (h, p), stained sections of primary motor cortex (M1, or area 4) (a–h), and the premotor area (PreM, or area 6) (i–p) of the African wild dog. In all images, the pial surface is to the top of the image. Layer demarcations are provided in (c) and (k) for each cortical area. Scale bar in (p) = 250 μm and applies to all.

3 | Results

The motor system of the African wild dog is composed of cortical territories, fiber tracts, and nuclear complexes, which are, in general, very similar to that observed in other carnivore and mammalian species. Here, we provide a systems-level description of the motor system of the African wild dog brain that includes the motor areas of the cerebral cortex, the motor nuclei of the dorsal thalamus, the striatopallidal complex and associated nuclei, cerebellum, red nucleus, the descending motor pathways including the pyramidal tract, the inferior olivary nuclear complex, the cranial nerve motor nuclei, and the ventral horn of the cervical spinal cord. We note that while we employed a range of immunohistochemical stains, to be succinct we report only those stains that revealed specific features relating the organization of the motor system.

3.1 | Motor Areas of the Cerebral Cortex

Our cyto-, myelo-, and chemoarchitectural analysis of the motor region of the cerebral cortex in the African wild dog revealed

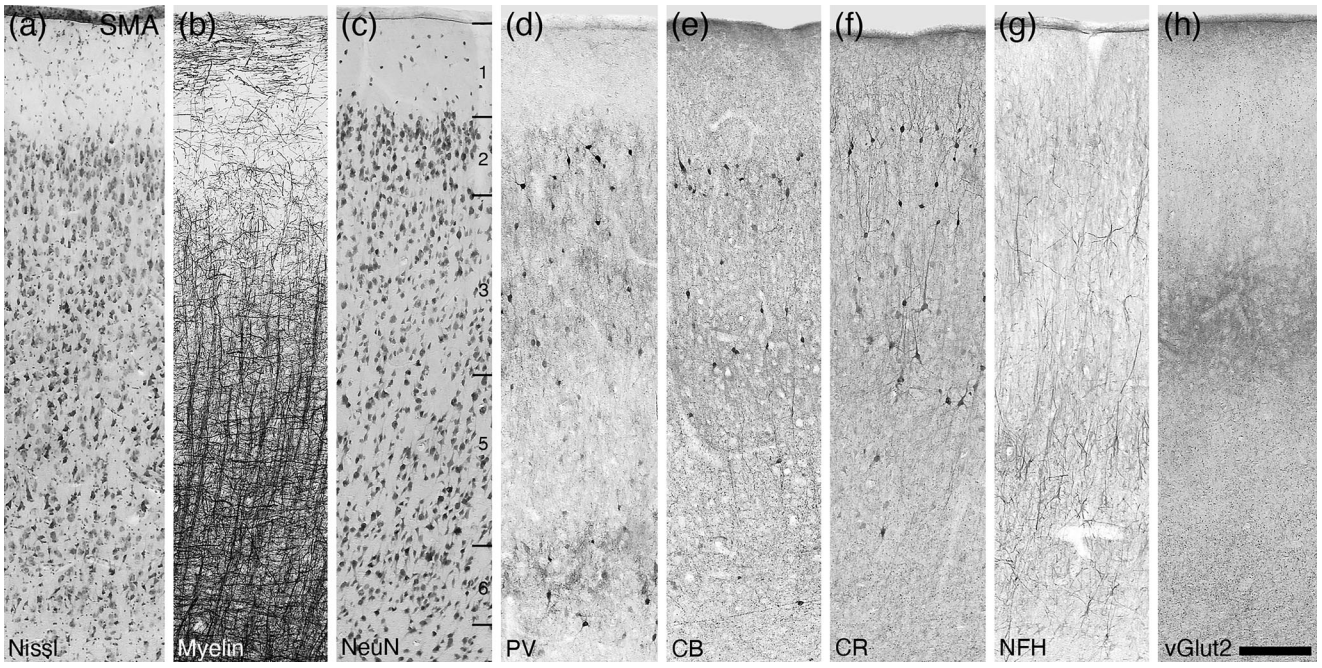

FIGURE 4 | Photomicrographs of Nissl (a), myelin (b), neuronal nuclear marker (NeuN) (c), parvalbumin (PV) (d), calbindin (CB) (e), calretinin (CR) (f), neurofilament H (NFH) (g), and vesicular glutamate transporter 2 (vGlut2) (h), stained sections of the supplementary motor area (SMA) of the African wild dog. In all images, the pial surface is to the top of the image. Layer demarcations are provided in (c). Scale bar in (h) = 250 μm and applies to all.

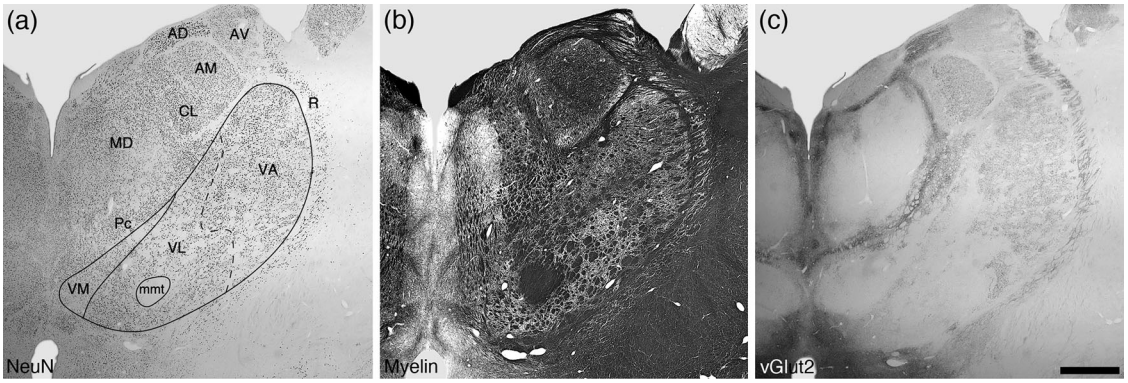

FIGURE 5 | Photomicrographs of adjacent coronal sections through the ventral lateral nuclear complex of the dorsal thalamus of the African wild dog stained with (a) neuronal nuclear marker (NeuN), (b) myelin, and (c) vesicular glutamate transporter 2 (vGlut2). Note the presence of the ventral anterior nucleus (VA), which is distinguished from the ventral lateral nucleus (VL) based on the VA having a distinct vGlut2 immunostaining (c). The mammillothalamic tract (mmt) passes through the VL, and at certain levels distinguishes the VL from the principal ventromedial nucleus of the thalamus (VM, which is part of the intralaminar nucleus complex). The VA and VL thalamic motor nuclei are bordered ventrolaterally by the external medullary lamina and the thalamic reticular nucleus (R), dorsally by the anteroventral (AV) and anteromedial nucleus of the thalamus (AM), and dorsomedially by the paracentral (Pc) and central lateral nuclei of the thalamus (CL). Other thalamic nuclei labeled in (a) include the anterodorsal nucleus of the thalamus (AD) and the mediodorsal nucleus of the thalamus (MD). Scale bar in (c) = 2 mm and applies to all.

the presence of three cortical areas that were located on the anteromedial surface of the cortical mantle (Figures 1 and 2). The motor cortical areas were located deep within the cruciate sulcus (Figure 2g,h) and rostral to the cruciate sulcus on the anterior sigmoid gyrus and the caudal portion of the frontal gyrus (including the mesial wall) (Figures 1 and 2). All three cortical areas were composed of five cortical layers, with no cytoarchitecturally distinct layer 4 being noted. The three distinct cortical areas include the primary motor cortex (M1, or Brodmann area 4), the premotor cortical area (PreM, or Brodmann area 6), and the supplementary motor area (SMA), all located rostral to somatosensory area 3a (Chengetanai et al. 2025).

3.1.1 | Primary Motor Cortex (M1/Area 4)

Neurons were observed in all cortical layers, with layer 1 showing the lowest neuronal density, while layer 2 exhibited the highest density and was composed of smaller granular neurons. A relatively lower density of pyramidal neurons was observed

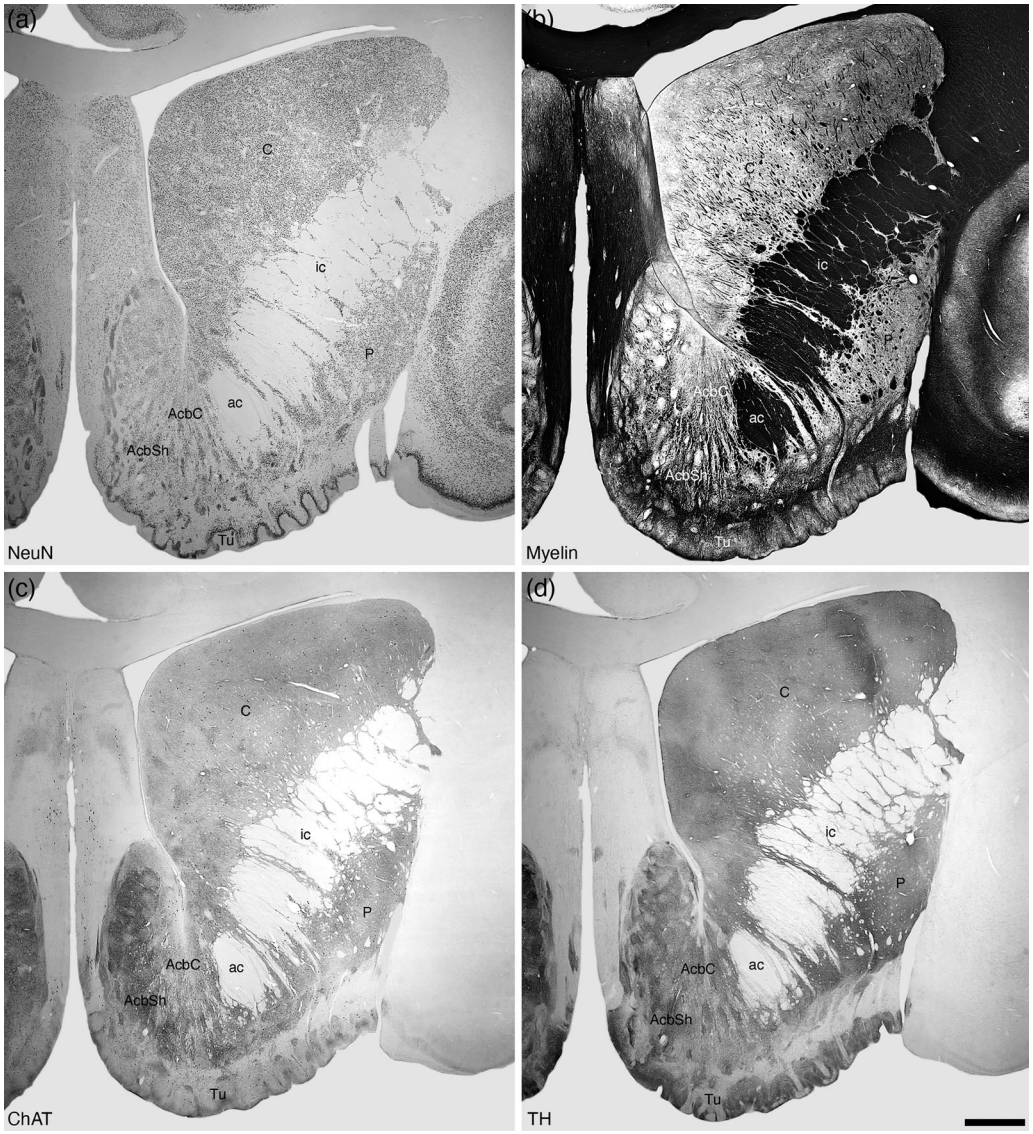

FIGURE 6 | Photomicrographs of adjacent coronal sections through portions of the striatopallidal complex of the African wild dog stained with (a) neuronal nuclear marker (NeuN), (b) myelin, (c) choline acetyltransferase (ChAT), and (d) tyrosine hydroxylase (TH). The caudate (C) and putamen (P) are clearly separated by a distinct internal capsule (ic). At the ventromedial edge of these three structures, demarcated by the anterior commissure (ac), we identified the core (AcbC) and shell (AcbSh) portions of the nucleus accumbens. Ventrally adjacent to the nucleus accumbens, the distinct olfactory tubercle (Tu) was observed. In all images, medial is to the left and dorsal to the top. Scale bar in (d) = 2 mm and applies to all.

through the relatively thick layers 3 and 5, with layer 5 being distinct due to the presence of gigantocellular pyramidal (or Betz) neurons. Neuronal density was higher in layer 6, with the neurons exhibiting a range of soma shapes (Figure 3a,c). A moderate density of myelinated fibers was observed through all layers, with layer 1 revealing numerous horizontally oriented fibers, a distinct sparsity of myelinated fibers in layer 2, with a mix of horizontally oriented fibers and thin, weakly aggregated radial fascicles extending from layer 6 through to layer 2 (Figure 3b).

Parvalbumin-immunostaining revealed neurons in layers 2–6, with a heterogeneous neuropil staining, being most dense in layer 5, followed by layer 2 and outer layer 3, with inner layer 3 and layer 6 showing the least dense neuropil staining (Figure 3d). Calbindin-immunostaining revealed neurons in layers 2–6, with the greatest density being observed in layer 2, followed by layer 5, with layers 3 and 6 only having the occasional immunopositive neuron. The calbindin-immunopositive neuropil staining throughout all cortical layers, from 1 to 6, was homogenous (Figure 3e). Calretinin-immunopositive neurons were observed mostly in layer 2 with the occasional neuron being observed in layer 3. Calretinin-immunopositive neuropil staining was noted in all cortical layers, from 1 to 6, with a slightly higher density of immunopositive structures being observed in layers 1–3 (Figure 3f). Neuronal structures immunopositive to neurofilament H were observed in all layers, with prominent staining of the gigantopyramidal neurons in layer 5, and the apical dendrites of pyramidal neurons of layers 5 and 3 clearly labeled. Occasional neurofilament H-immunopositive neurons were observed in layers 2 and 3 (Figure 3g). The greatest density of vesicular glutamate transporter 2-immunostained boutons was observed in the inner

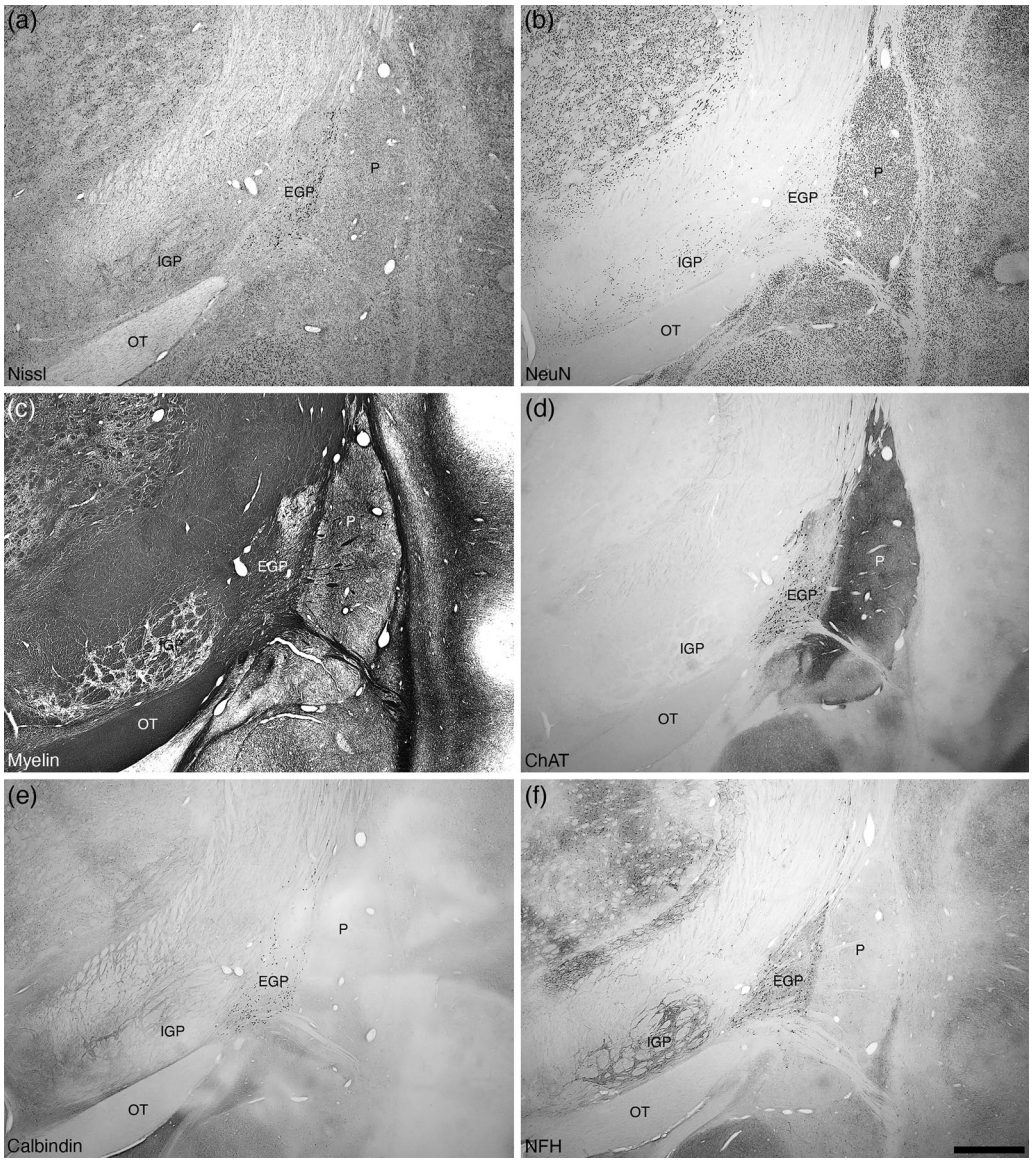

FIGURE 7 | Photomicrographs of adjacent coronal sections through the globus pallidus of the African wild dog stained with (a) Nissl, (b) neuronal nuclear marker (NeuN), (c) myelin, (d) choline acetyltransferase (ChAT), (e) calbindin, and (f) neurofilament H (NFH). Both the external (EGP) and internal (IGP) divisions of the globus pallidus are readily identifiable in the African wild dog, located ventromedial to the putamen (P), at the level of the optic tract (OT). In particular, the ChAT (d), calbindin (e), and NFH (f) stains reveal the EGP, while the NeuN (b), myelin (c), and NFH (f) stains clarify the location and extent of the IGP. In all images, medial is to the left and dorsal to the top. Scale bar in (f) = 2 mm and applies to all.

portion of layer 3, with moderate-to-low densities observed in layers 1 and 6, although these boutons were observed in all cortical layers (Figure 3h).

3.1.2 | Premotor Cortex (PreM/Area 6)

Neurons were observed in all cortical layers, with layer 1 showing the lowest neuronal density, while the granular layer 2 exhibited the highest neuronal density. A slightly lower density of pyramidal neurons was observed through the relatively thick layers 3 and 5, with layer 5 revealing the very occasional gigantocellular pyramidal (or Betz) neuron. Neuronal density was similar in layer 6, with the neurons exhibiting a range of somal shapes. A moderate-to-high density of myelinated fibers was observed through all layers, with layer 1 revealing numerous, loosely arranged, horizontally oriented fibers, a distinct sparsity of myelinated fibers in layer 2, with a mix of horizontally oriented fibers and with radial fascicles, being thicker than observed in M1, extending from layer 6 through to layer 3 (Figure 3j).

Parvalbumin-immunostaining revealed neurons in layers 2–6, with most of these neurons being observed in layer 3. A heterogeneous neuropil staining was noted, being most dense in layer 5, followed by layer 2 and outer layer 3, with inner layer 3 and layer 6 showing the least dense neuropil staining (Figure 3l). Calbindin-immunostaining revealed neurons in layers 2, 3, and 5, with the greatest density being observed in layer 2, followed by layers 3 and 5. Calbindin-immunopositive neuropil staining throughout all cortical layers, from 1 to 6, was homogenous

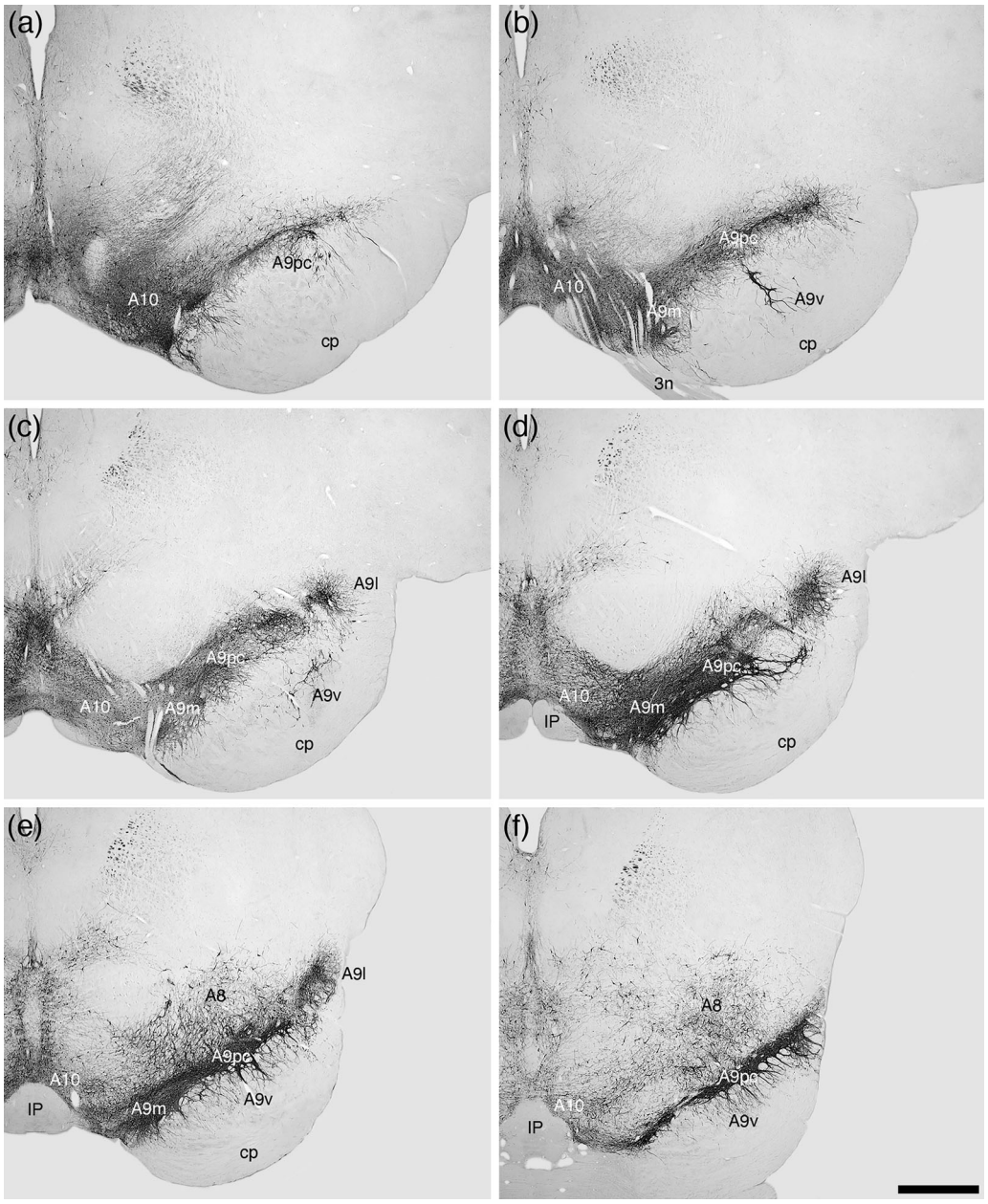

FIGURE 8 | Photomicrographs of serial coronal sections, (a) being the most rostral section, (f) the most caudal (each section being 1 mm apart), through the substantia nigra nuclear complex of the African wild dog revealed with tyrosine hydroxylase immunohistochemistry. The substantia nigra nuclear complex in the African wild dog was composed of the medial (A9m), pars compacta (A9pc), lateral (A9l), and ventral (A9v) subdivisions. In addition, though not described in detail herein, we note the ventral tegmental area (the A10 complex) and the retrorubral nucleus (A8). In all images, medial is to the left and dorsal to the top. Scale bar in (f) = 2 mm and applies to all. 3n—oculomotor nerve, IP—interpeduncular nucleus, cp—cerebral peduncle.

(Figure 3m). Calretinin-immunopositive neurons were observed in all cortical layers, with the highest density noted in layer 2 with the occasional neuron being observed in layer 6. Calretinin-immunopositive neuropil staining was homogeneous throughout layers 1–6 (Figure 3n). Neuronal structures immunopositive to neurofilament H were observed in all layers, with the highest density of immunostained structures being observed in layers 5 and 6 (Figure 3o). The greatest densities of vesicular glutamate transporter 2-immunostained boutons were observed in layer 1 and the inner portion of layer 3, with moderate densities observed in layer 6, with boutons being observed in all cortical layers (Figure 3p).

3.1.3 | Supplementary Motor Area

Neurons were observed in all cortical layers, with layer 1 showing the lowest neuronal density, while the small, pyramidalized, neurons of layer 2 exhibited the highest density. A slightly lower density of pyramidal neurons was observed through the relatively thick layers 3 and 5. Neuronal density was similar in layer 6 (Figure 4a,c), with the neurons exhibiting a range of somal shapes. A moderate-to-high density of myelinated fibers was observed through all layers, with layer 1 revealing numerous, loosely arranged, horizontally oriented fibers in its outer portion,

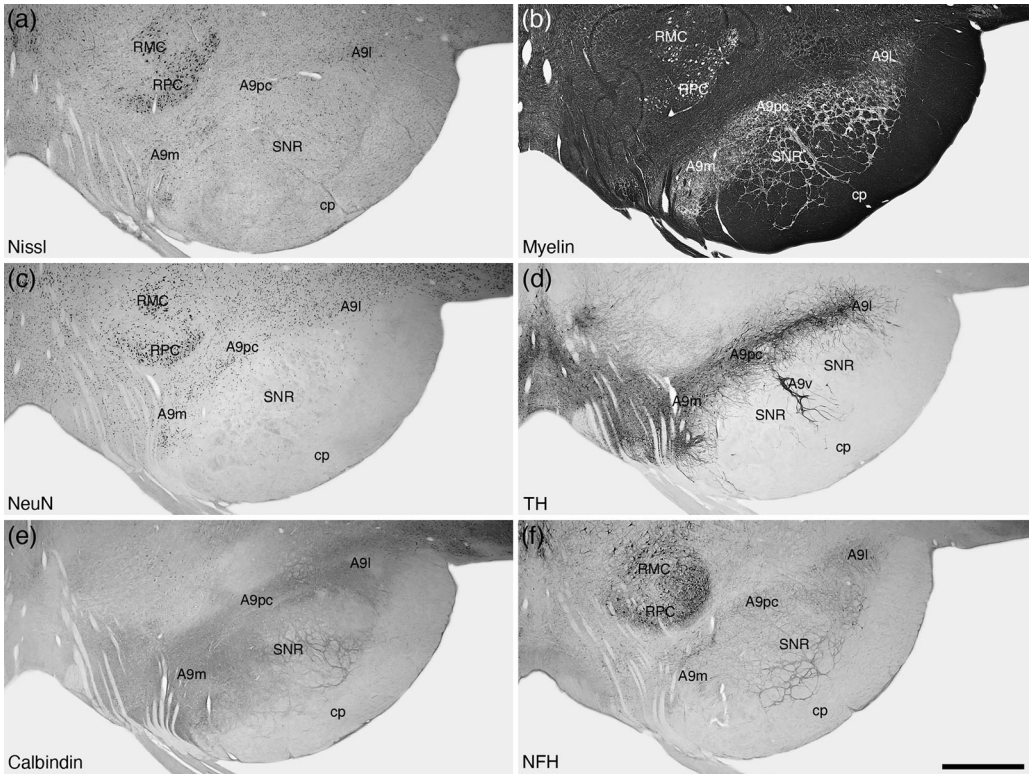

FIGURE 9 | Photomicrographs of adjacent coronal sections through the substantia nigra, pars reticulata (SNR) of the African wild dog stained with (a) Nissl, (b) myelin, (c) neuronal nuclear marker (NeuN), (d) tyrosine hydroxylase, (e) calbindin, and (f) neurofilament H (NFH). The SNR was located between the nuclei forming the substantia nigra nuclear complex and the cerebral peduncle (cp). A low neuronal density with a reticulated appearance was noted in this ellipsoid-shaped nucleus. In all images, medial is to the left and dorsal to the top. Scale bar in (f) = 2 mm and applies to all. A9l—substantia nigra, lateral, A9m—substantia nigra, medial, A9pc—substantia nigra, pars compacta, A9v—substantia nigra, ventral, RMC—red nucleus, magnocellular part, RPC—red nucleus, parvicellular part.

a distinct sparsity of myelinated fibers in layer 2, with a mix of horizontally oriented fibers and with radial fascicles, being more distinct than in M1 or PreM, extending from layer 6 through to layer 3 (Figure 4b).

Parvalbumin-immunostaining revealed neurons in layers 2–6, with the highest density of these neurons being observed in layer 2, with occasional neurons observed in layers 3 and 6, and very few observed in layer 5. A heterogeneous neuropil staining was noted, with this being most dense in layer 6, followed by layers 2 and 3, with layer 5 showing the least dense neuropil staining (Figure 4d). Calbindin-immunostaining revealed neurons in layers 2, 3, and 6, with the greatest density being observed in layer 2, followed by layer 3, with the very occasional neuron noted in layer 6. The calbindin-immunopositive neuropil staining throughout all cortical layers, from 1 to 6, was homogenous (Figure 4e). Calretinin-immunopositive neurons were observed in layers 2–6, with the highest densities noted in layers 2 and 3 with the occasional neuron being observed in layers 5 and 6. Calretinin-immunopositive neuropil staining was homogeneous throughout layers 1–6 (Figure 4f). Neuronal structures immunopositive to neurofilament H were observed in all layers, with the highest density of immunostained structures being observed in layers 3, 5, and 6 (Figure 4g). The greatest density of vesicular glutamate transporter 2-immunostained boutons was observed in the inner portion of layer 3, with boutons being observed in all cortical layers (Figure 4h).

3.2 | Motor Nuclei of the Dorsal Thalamus—The Ventral Lateral Nuclear Group

We identified the ventral anterior (VA) and ventral lateral (VL) nuclei (Figure 5) in the rostral, ventral, and lateral aspects of the gray matter mass that forms the dorsal thalamus. These nuclei were bordered ventrally and laterally by the external medullary lamina and thalamic reticular nucleus, dorsolaterally by the central lateral and the anterior nuclei, and dorsomedially by the central lateral, paracentral, and principal ventromedial nuclei (Figure 5), revealing a position within the dorsal thalamus typical of carnivores (Jones 2007).

The border distinguishing the VA and VL was not always readily apparent and is only tentatively marked (Figure 5a). Both the VA and VL exhibit a moderate neuronal density (relative to surrounding structures), although the neuronal density appears somewhat higher in the VA (Figure 5a). Both the VA and VL have numerous myelinated fascicles that traverse the nucleus, although the size and density of these myelin fascicles are higher in VL than VA (Figure 5b). The mammillothalamic tract was observed to traverse the VL, and at certain levels distinguished the VL from the principal ventromedial nucleus of the thalamus (which is part of the intralaminar nuclear complex) (Figure 5b). A moderate density of neural structures immunolabeled for vesicular glutamate transporter 2 was observed in the VA, whereas these structures were far less dense in the VL (Figure 5c). This vesicular

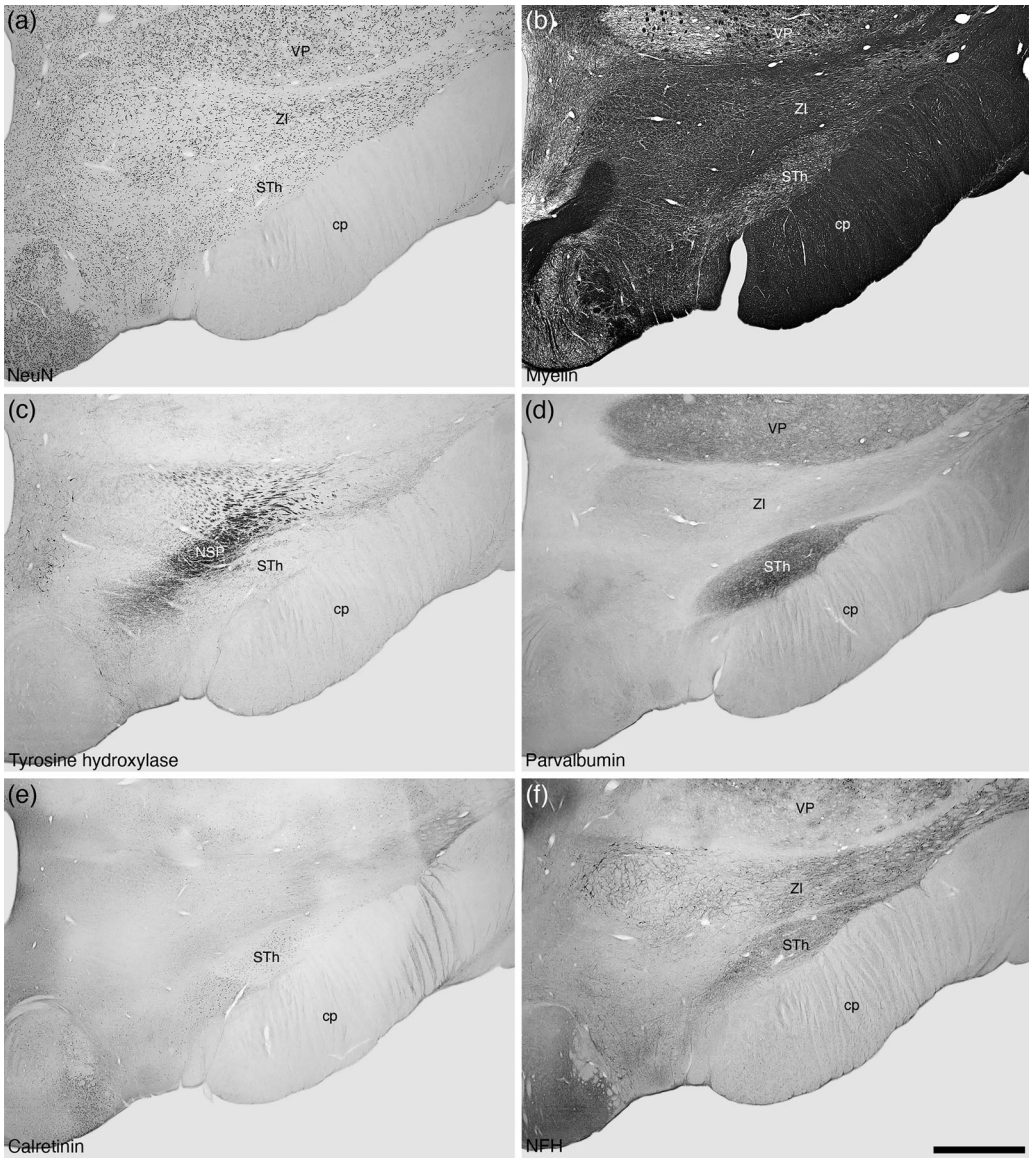

FIGURE 10 | Photomicrographs of adjacent coronal sections through the subthalamic nucleus (STh) of the African wild dog stained with (a) neuronal nuclear marker (NeuN), (b) myelin, (c) tyrosine hydroxylase, (d) parvalbumin, (e) calretinin, and (f) neurofilament H (NFH). The STh in the African wild dog is bordered ventrolaterally by the cerebral peduncle (cp), dorsally by the zona incerta (ZI), and dorsomedially by the nigrostriatal projection (NSP), a position typically seen across mammals. The location and extent of the STh are most clearly revealed by intense parvalbumin neuropil immunoreactivity (d) and NFH (f) immunoreactivity, but also contains calretinin immunopositive neurons (e). In all images, medial is to the left and dorsal to the top. Scale bar in (f) = 2 mm and applies to all. VP—ventral posterior thalamic nuclear complex.

glutamate transporter 2-immunolabelling provided the clearest distinction between the VA and VL nuclei.

3.3 | Striato-Pallidal Complex

The striatopallidal complex of the African wild dog was composed of dorsal and ventral complexes. Within the dorsal striatopallidal complex, we identified the caudate/putamen and the external globus pallidus and internal globus pallidus (also known as intrapeduncular and entopeduncular nuclei). The ventral striatopallidal complex was composed of the nucleus accumbens and olfactory tubercle. Nuclei associated with the striatopallidal complex include the midbrain dopaminergic neurons of the ventral tegmental area (A10) and the substantia nigra (A9), as well as the subthalamic nucleus and superior colliculus.

3.3.1 | Dorsal Striatopallidal Complex

The location of the dorsal striatopallidal complex in the brain of the African wild dog has been outlined previously (see fig. 7 in Chengetanai et al. 2020a) and occupies a position typically observed in mammals. The rostral pole of the caudate/putamen becomes divided into dorsomedial (caudate nucleus) and ventrolateral (putamen nucleus) parts by the passage of the distinct internal capsule (Figure 6). Thin bridges of neurons traverse the internal capsule (Figure 6a). The neuronal density of the caudate

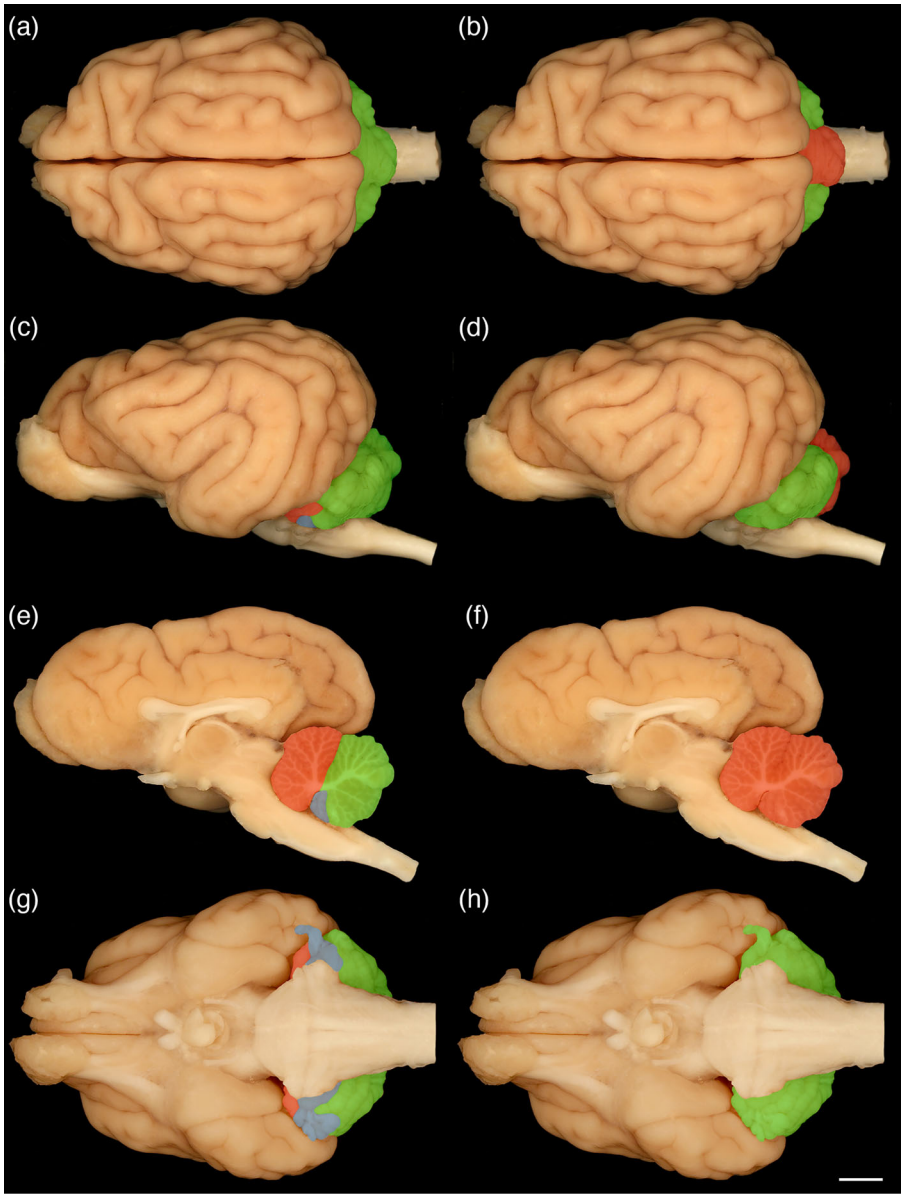

FIGURE 11 | Photographs of the brain of the African wild dog in dorsal (a, b), lateral (c, d), mid-sagittal (e, f), and ventral (g, h) views showing the anatomical (a, c, e, g) and functional (b, d, f, h) subdivisions of the cerebellum. (a, c, e, g) The anterior lobe is shaded in red, the posterior lobe in green, and the flocculonodular lobe in blue. (b, d, f, h) The vermal, the presumed spinal recipient region, is shaded in red, and the hemispheric, the presumed pontine recipient region, shaded in green. In all images, rostral is to the left. Scale bar in h = 1 cm and applies to all.

and putamen is moderately high, but homogeneous and similar in density throughout both nuclei. The myelinated fibers within these nuclei show a similar homogeneity, although the dorsomedial aspect of the caudate nucleus appears to have less myelin fascicles (Figure 6b). Choline acetyltransferase-immunopositive neurons were observed in both nuclei, with a homogeneous density and distribution throughout these nuclei. The intense neuropil immunostaining for both choline acetyltransferase and tyrosine hydroxylase was relatively homogeneous throughout both nuclei (Figure 6c,d).

At the caudal end of the putamen nucleus, we could readily identify both the external globus pallidus (EGP) and the internal globus pallidus (IGP) (Figure 7). The moderately myelin dense EGP was located ventromedially adjacent to the putamen nucleus and contained a moderate density of choline acetyltransferase-, calbindin-, and neurofilament H-immunoreactive neurons (Figure 7). Moderately intense choline acetyltransferase- and neurofilament H-immunoreactive neuropil staining was observed in the EGP. Ventromedial to the EGP, lying dorsal to the optic tract, a similar density of neurons was designated at the IGP. The neurons of the IGP were distributed around large myelin fascicles that traversed this nucleus. IGP neurons were not immunopositive for choline acetyltransferase, but a distinct neurofilament-H-neuropil immunostaining was observed throughout the IGP (Figure 7).

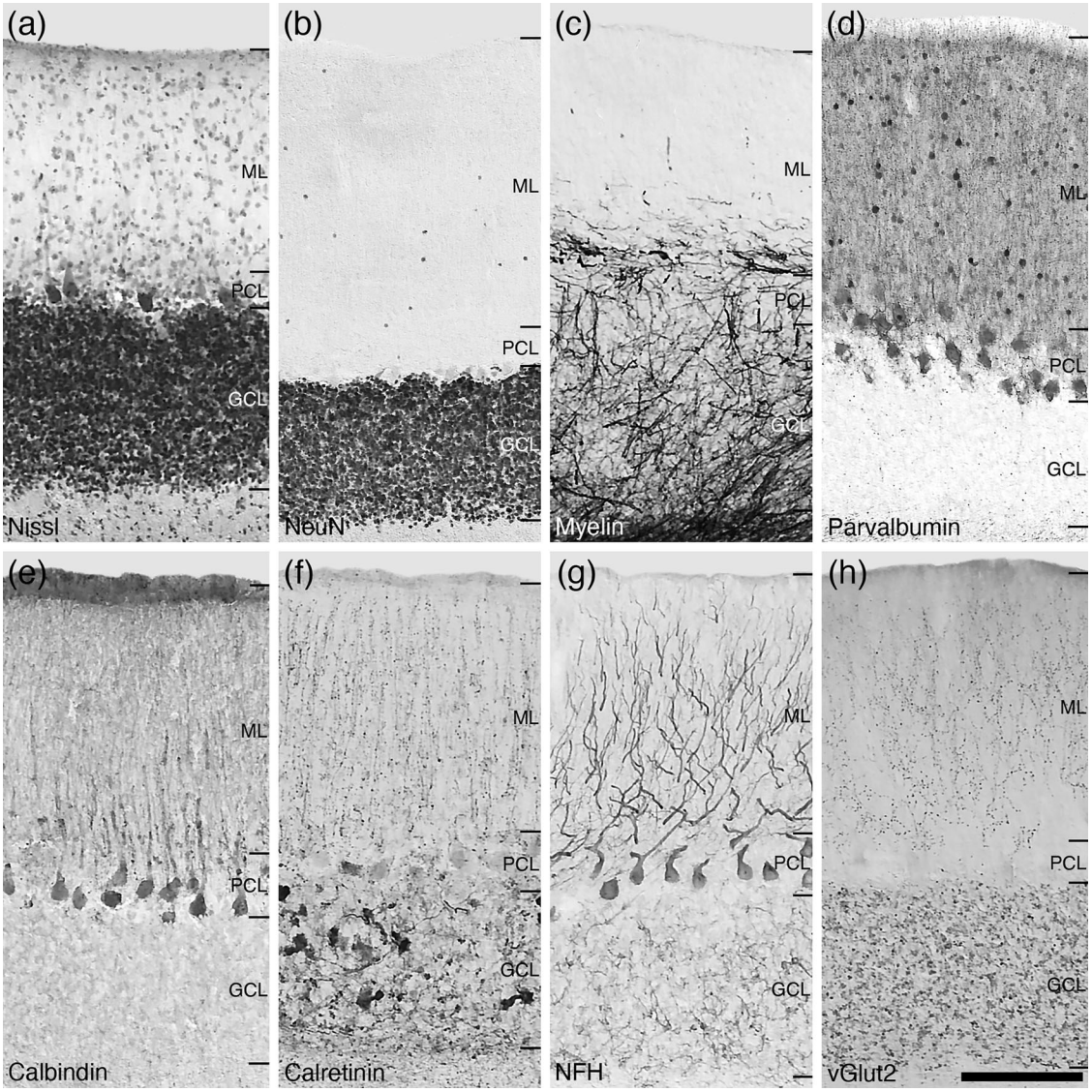

FIGURE 12 | Photomicrographs of coronal sections through the cerebellar cortex of the African wild dog stained with (a) Nissl, (b) neuronal nuclear marker (NeuN), (c) myelin, (d) parvalbumin, (e) calbindin, (f) calretinin, (g) neurofilament H (NFH), and (h) vesicular glutamate transporter 2 (vGlut2). The three layers of the cerebellar cortex, the molecular layer (ML), Purkinje cell layer (PCL), and granule cell layer (GCL), typical of mammals are present. In all images, the pial surface is to the top. Scale bar in (h) = 250 μm and applies to all.

3.3.2 | Ventral Striatopallidal Complex

The nucleus accumbens of the African wild dog is located in the region typically observed in mammals, ventral and medial to the lateral ventricle, and ventral to the anterior commissure. The nucleus accumbens is typically described as being composed of a core and a shell (e.g., Meredith et al. 1992). The core of the nucleus accumbens contained a moderately neuron density, formed by weakly striated radially arranged neuronal clusters separated by loosely aggregated myelinated fascicles (Figure 6a,b). The intense neuropil immunostaining for both choline acetyltransferase and tyrosine hydroxylase was relatively homogeneous in the core of the nucleus accumbens (Figure 6c,d). Choline acetyltransferase-immunopositive neurons were distributed throughout the core of the nucleus accumbens.

The core of the nucleus accumbens was bordered, ventrally and medially, by a distinct patchy region of neurons and myelin that we designate as the shell of the nucleus accumbens (Figure 6a,b). This heterogeneous clustering of neurons and myelin was also noted for the intense neuropil immunostaining revealed with choline acetyltransferase and tyrosine hydroxylase antibodies (Figure 6c,d). Choline acetyltransferase-immunopositive neurons were distributed throughout the shell of the nucleus accumbens, although in slightly lower density than seen in the core. Bordering the ventral and lateral aspects of the shell of the nucleus accumbens, several clusters of neurons, presumably the islands of Calleja, formed a third layer in this region. The heterogeneous appearance of the islands of Calleja was also observed with the intense neuropil immunostaining for both choline acetyltransferase and tyrosine hydroxylase (Figure 6). The location and neurochemistry of the olfactory tubercle has been

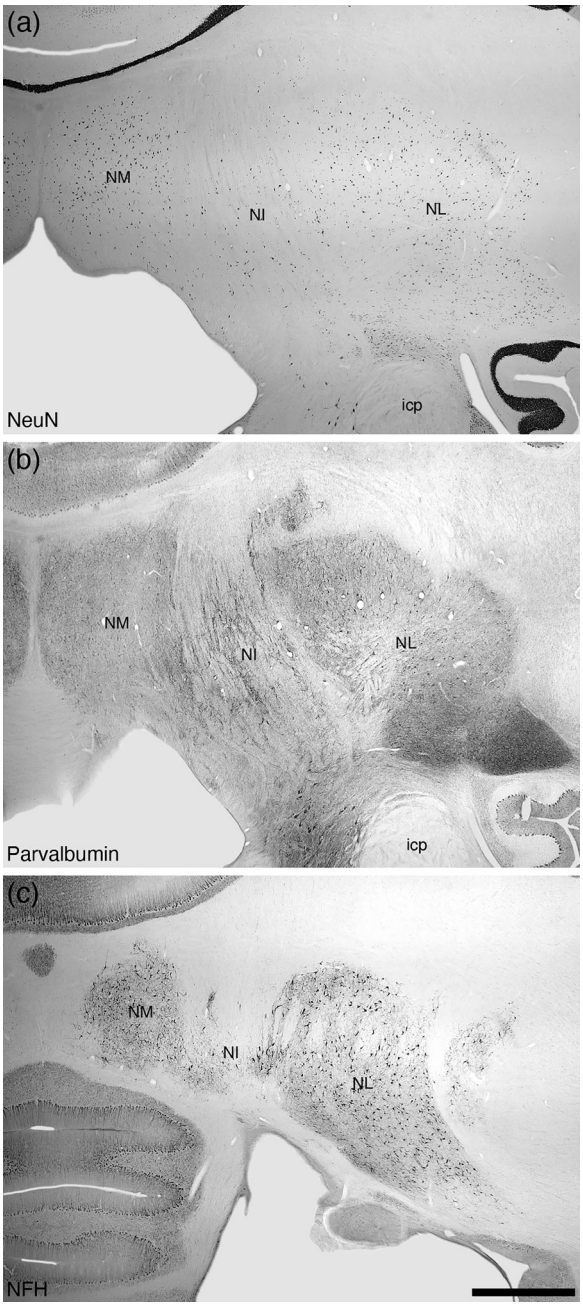

FIGURE 13 | Photomicrographs of coronal sections through the cerebellar nuclei of the African wild dog immunostained with (a) neuronal nuclear marker (NeuN), (b) parvalbumin, and (c) neurofilament H (NFH). Note the presence of three distinct cerebellar nuclei, the medial (NM), interpositus (NI), and lateral (NL) nuclei, lying in a position dorsal to the inferior cerebellar peduncle (icp). In all images, dorsal is to the top and medial to the left. Scale bar in (h) = 250 μm and applies to all.

described in detail previously (Chengetanai et al. 2020b) and is not described further herein (Figure 6).

3.3.3 | Associated Nuclei

Immunostaining for tyrosine hydroxylase revealed the ventral tegmental area (A10) and substantia nigra complex (A9) (Figure 8). The neurons forming the A10 were located close to the ventral midline of the midbrain, medial to the root of the oculomotor nerve, with small clusters of A10 neurons observed ventral to the cerebral aqueduct. The A9 complex formed a distinct band of densely packed neurons lying medial and dorsal to the upper border of the substantia nigra, reticular part (SNR), lateral to the root of the oculomotor nerve. The A9 of the African wild dog could be readily parcellated into medial (A9m), pars compacta (A9pc), lateral (A9l), and ventral (A9v, nestled within the SNR) parts (Figure 8). A full description of these nuclei will be provided in a subsequent study.

Located between the A9 and the cerebral peduncle, the substantia nigra, reticular part (SNR) formed a distinct ellipsoid-shaped nucleus (the long axis of this ellispe oriented in a dorsolateral-ventromedial plane) (Figure 9). Within the SNR, a low density of neurons was observed (Figure 9c), intermingled with relatively large fascicles of myelinated axons that appear to be part of the cerebral peduncle (Figure 9b). Tyrosine hydroxylase neurons of the A9v were invested into these inter-fascicular regions (Figure 9d). The neurons of the SNR have been reported to be primarily GABAergic (e.g., Partanen and Achim 2022); however, we found no evidence of immunopositivity of the neurons of the SNR to parvalbumin, calbindin (Fig. 9e), or calretinin antibodies. The reticulated appearance of the SNT is highlighted by both myelin and neurofilament H stains (Figure 9b,f).

The subthalamic nucleus was located dorsal to the cerebral peduncle (rostral to the A9), and ventral to the zona incerta and the nigrostriatal projection, at the level of the mammillary bodies (Figure 10). This mediolaterally compressed nucleus was readily demarcated with neuronal nuclear marker-immunostaining, a relatively lower density of myelinated fibers, an intense parvalbumin-neuropil immunostaining, a very pale calretinin-neuropil immunostaining, and a distinct neurofilament H-immunostaining (Figure 10). The location of this nucleus is like that observed in other mammals. The location and neurochemistry of the deep layers of the superior colliculus have been described in detail previously (Chengetanai et al. 2020d) and are not described further herein.

3.4 | Cerebellum

The cerebellum of the African wild dog was located caudal to the cerebral hemispheres, and dorsal to the brainstem in the standard position for mammals (Figure 11). The African wild dog cerebellum exhibited the typical vermal and hemispheric portions and could be divided into anterior, posterior, and flocculonodular lobes (Figure 11), none of which revealed proportions differing substantively to that observed in many other mammals. The anterior and posterior lobes were separated by a distinct primary fissure, while the flocculus was evident in gross examination and the nodulus (vermian lobule X) in the hemi-sected brain (Figure 11). The vermian lobules typically observed in mammals were also readily identified in the African wild dog and include I—lingula; II, III—centralis; IV, V- culmen; VI—declive, VII—folium and tuber vermis; VIII—pyramis; IX—Uvula; X—nodulus (see Figure 3b of Chengetanai et al. 2020a). Distinct superior, middle, and inferior cerebellar peduncles were also observed connecting the cerebellum with the midbrain, pons, and medulla oblongata, respectively.

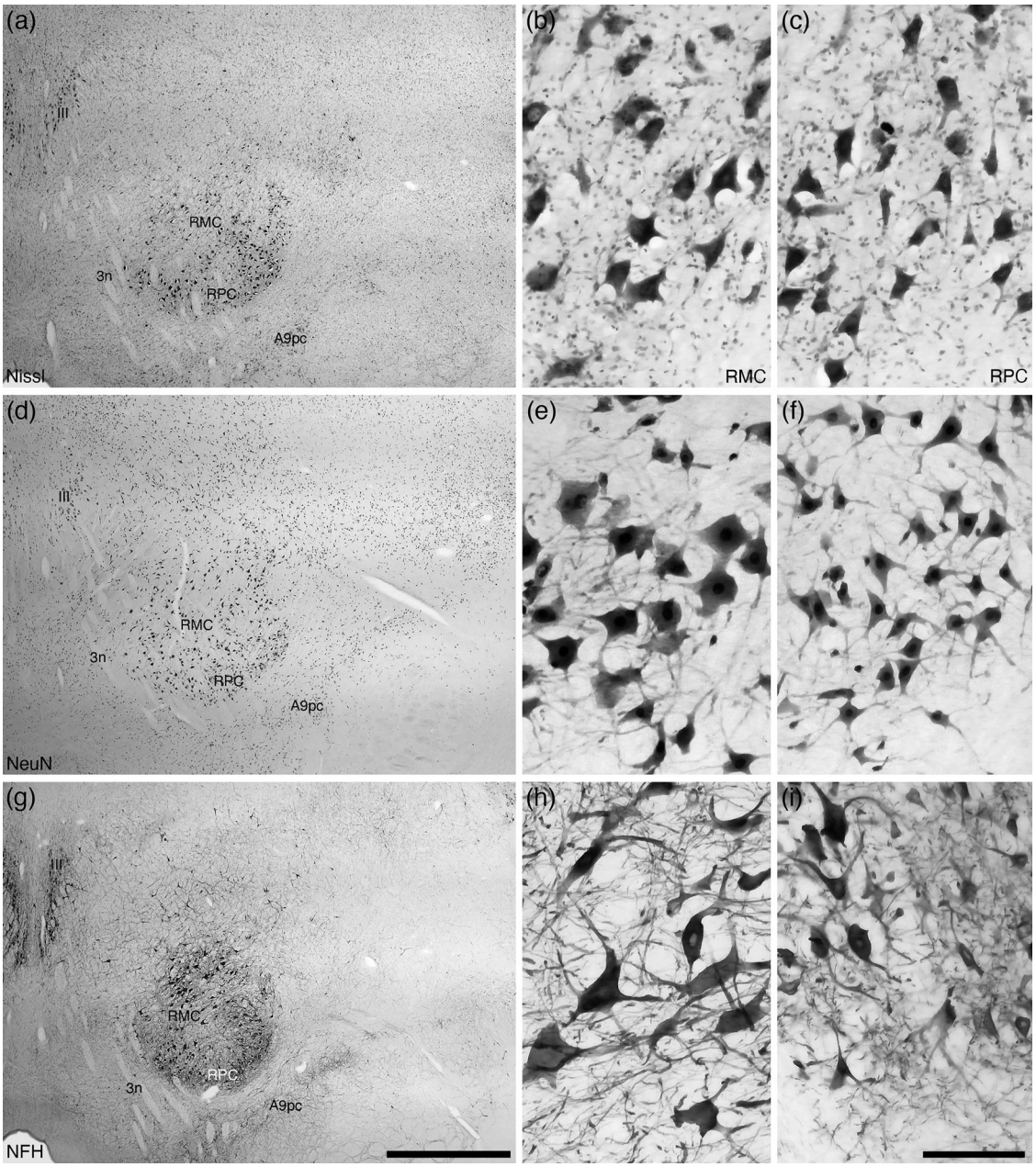

FIGURE 14 | Low (a, d, g) and higher (b, c, e, f, h, i) magnification photomicrographs of coronal sections through the red nucleus of the African wild dog stained with (a, b, c) Nissl, (d, e, f) neuronal nuclear marker (NeuN), and (g, h, i) neurofilament H (NFH). These stains reveal both the magnocellular (RMC) and parvicellular (RPC) parts of the red nucleus, the RPC lying ventrolateral to the RMC. As is typical for mammals, the red nucleus is found ventrolateral to the oculomotor nucleus (III) in the midbrain tegmentum, immediately lateral to the roots of the oculomotor nerve (3n) and dorsal to the substantia nigra, pars compacta (A9pc). The neurons forming the RMC (b, e, h) are clearly larger than those forming the RPC (c, f, i). In all images, medial is to the left and dorsal to the top. Scale bar in (g) = 2 mm and applies to (a), (d) and (g). Scale bar in (i) = 150 μm and applies to (b), (c), (e), (f), (h), and (i).

3.4.1 | Cerebellar Cortex

The cerebellar cortex exhibited the typical trilaminate appearance of mammals (Bhagwandin et al. 2024), including, from superficial to deep, the molecular, Purkinje cell, and granular layers (Figure 12). The neuron sparse molecular layer revealed stellate and basket and cells that were immunopositive for parvalbumin (Figure 12d). At the border between the molecular and Purkinje cell layer, a dense network of horizontally oriented myelinated axons was observed (Figure 12b). Climbing fibers were revealed with both calretinin- and vesicular glutamate transporter 2-immunostaining (Figure 12f,h), while the dendrites of Purkinje cells were clearly revealed with neurofilament H-immunostaining (Figure 12g).

A monolayer of the large Purkinje cells was revealed with Nissl staining, with these cells being moderately intensely immunostained with parvalbumin, calbindin, and neurofilament H (Figure 12d,e,g). Neuronal nuclear marker- and vesicular glutamate transporter 2-immunostaining did not reveal any structures

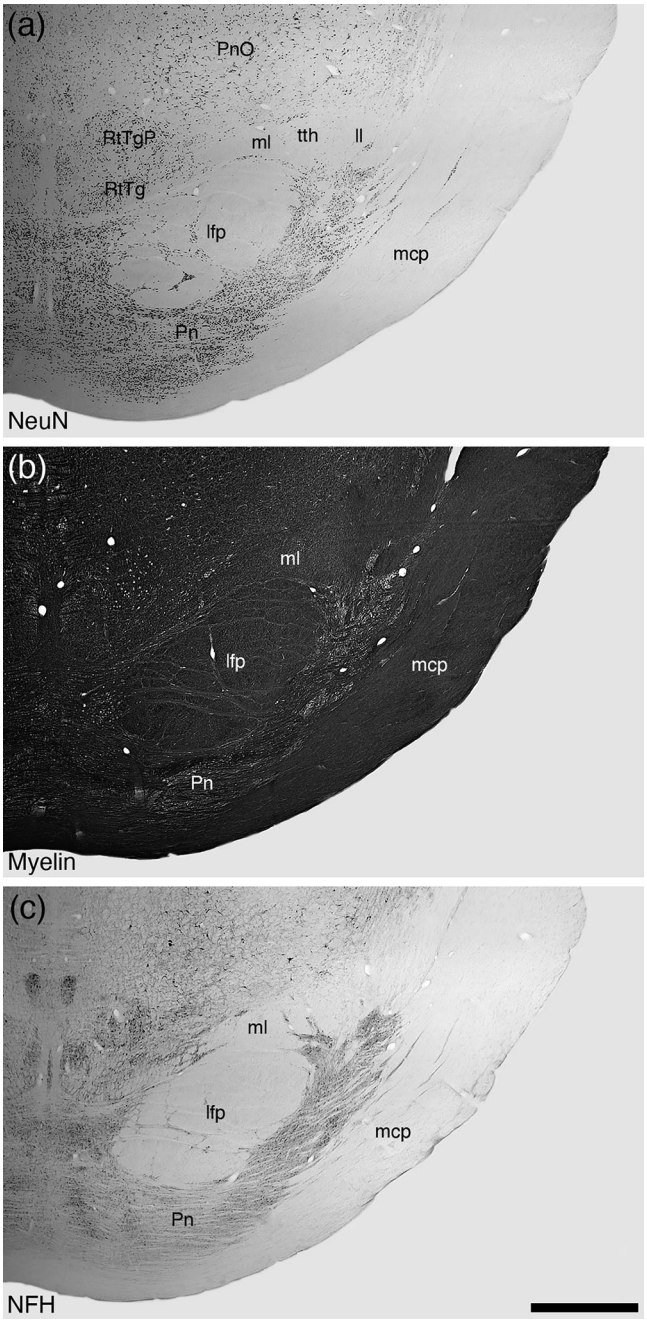

FIGURE 15 | Photomicrographs of adjacent coronal sections through the pontine nucleus (Pn) of the African wild dog stained with (a) neuronal nuclear marker (NeuN), (b) myelin, and (c) neurofilament H (NFH). The distinct longitudinal fasciculus of the pons (lfp) is encased within the Pn. Scale bar in (c) = 2 mm and applies to all. ll—lateral lemniscus; mcp—middle cerebellar peduncle; ml—medial lemniscus; PnO—oral part of the pontine reticular nucleus; RtTg—reticulotegmental nucleus of the pons; RtTgP—pericentral part of the reticulotegmental nucleus of the pons; tth—trigeminothalamic tract.

in the Purkinje cell layer (Figure 12b,h), and the density of myelinated fibers was lower in the Purkinje cell layer compared to the granule cell layer (Figure 12c). Parallel fibers adjacent to the Purkinje cells were revealed with parvalbumin-immunostaining (Figure 12d), with occasional calbindin-immunopositive terminals being observed on the soma and proximal dendrites of the Purkinje cells (Figure 12e).

The high neuronal density within the granular layer was clearly revealed with both Nissl and neuronal nuclear marker stains (Figure 12a,b). A moderate density of myelinated axons was observed in the granular layer, but parvalbumin- and calbindin-immunostaining did not reveal any neuronal structures in this layer (Figure 12c–e). Calretinin-immunostaining revealed granule cells, unipolar brush neurons (Figure 12f), Golgi type-II, and Lugaro neurons (not shown). A variety of neuronal structures were revealed with both neurofilament H- and vesicular glutamate transporter 2-immunostaining (Figure 12g,h).

3.4.2 | Cerebellar Nuclei

Immunostaining for neuronal nuclear marker, parvalbumin, and neurofilament H revealed the presence of three distinct cerebellar nuclei, the medial (NM), interpositus (NI), and lateral (NL), lying in a position dorsal to the inferior cerebellar peduncle (icp) (Figure 13). While the density and distribution of the neurons forming the NM and NL was quite similar and homogeneous, the NI has a far more heterogeneous appearance and a substantially lower neuronal density throughout the extent of this nucleus, presumably due to the passage of fibers emanating from the inferior cerebellar peduncle (Figure 13).

3.5 | Red Nucleus

The red nucleus of the African wild dog was situated in the mid-ventral aspect of the midbrain tegmentum at the level of the oculomotor nucleus (see Section 3.8). The red nucleus was located immediately lateral to the descending roots of the oculomotor nerve and dorsal to the substantia nigra (see Section 3.3.3) (Figure 14). Within the red nucleus, distinct magnocellular (RMC) and parvicellular (RPC) parts were readily identified, based on soma size, with Nissl, neuronal nuclear marker, and neurofilament H stains (Figure 14). The RMC, which contained distinctly larger multipolar soma, composed most of the red nucleus. The RPC, with distinctly smaller multipolar soma, was seen to form the ventrolateral portion of the red nucleus, although the border between the RMC and RPC showed intermingling of the larger and smaller neurons and is not a precise border (Figure 14).

3.6 | Cerebral Peduncle, Pontine Nucleus, and the Pyramidal Tract

The descending motor pathways arising from the cerebral cortex coalesced to form the distinct internal capsule that separates the caudate and putamen (Figure 6; see Sections 3.1 and 3.3). Ventrocaudal to the internal capsule, these fibers formed the distinct cerebral peduncle found ventrolateral to the subthalamic nucleus rostrally, and the substantia nigra caudally (see Figures 8–10 and Section 3.3.3). At the boundary between the midbrain and pons, a large proportion of these descending fibers terminated in the pontine nucleus, while others form the longitudinal fasciculus of the pons (Figure 15). The neurons forming the pontine nucleus, while being observed in high density, also showed a significant degree of heterogeneity due to the passage of the incoming fibers

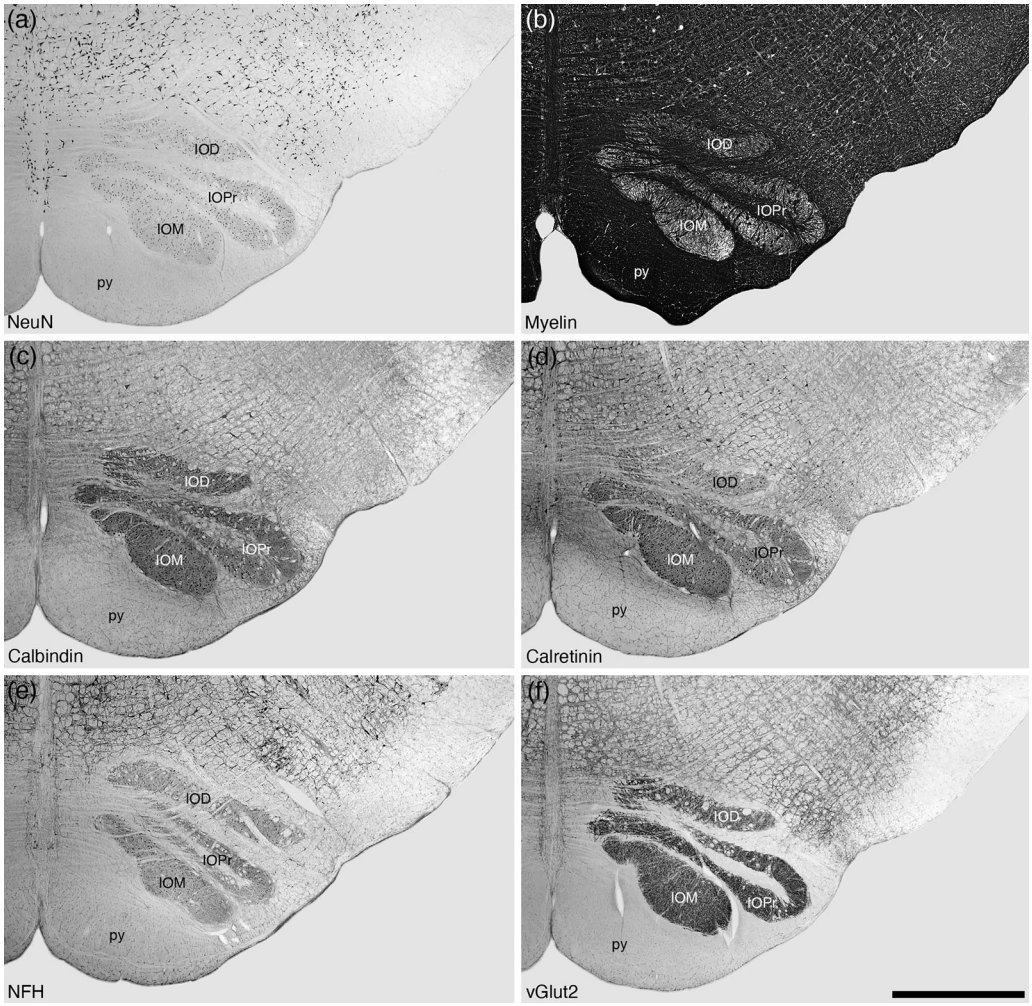

FIGURE 16 | Photomicrographs of adjacent coronal sections through the inferior olive nuclear complex of the African wild dog stained with (a) neuronal nuclear marker (NeuN), (b) myelin, (c) calbindin, (d) calretinin, (e) neurofilament H (NFH), and (f) vesicular glutamate transporter 2 (vGlut2). At the level depicted in this plate, three distinct nuclei of the inferior olive, the medial (IOM), principal (IOPr), and dorsal (IOD) nuclei, are readily observed with all stains. As is typical for mammals, the inferior olive is found dorsolateral to the pyramidal tract (py). In all images, medial is to the left and dorsal to the top. Scale bar in (f) = 2 mm and applies to all.

and those decussating and passing through this nucleus to the contralateral middle cerebellar peduncle. This heterogeneity was also readily observed with both myelin and neurofilament H stains (Figure 15).

The longitudinal fasciculus of the pons passes through the pontine nucleus, where at the border of the pons and medulla oblongata this fasciculus forms the distinct pyramidal tract. The myelin-dense pyramidal tract occupied the ventromedial aspect of the medulla oblongata throughout its rostro-caudal extent (Figures 11g,h and 16). At the spinomedullary junction, the fibers forming this tract form the decussation of the pyramidal tract, coursing dorsally and across the midline ventral to the central canal of the spinal cord (Figure 17a).

3.7 | Inferior Olivary Nuclear Complex

The inferior olivary nuclear complex, located in the ventromedial aspect of the rostral medulla oblongata dorsolateral to the pyramidal tract, was composed of the principal (IOPr), medial (IOM), and dorsal (IOD) nuclei of the inferior olive (Figure 16). These three nuclei showed the intercalated and sinusoidal appearance of the nuclei typical of the mammalian inferior olive, with the same topological relationships to one another observed in other mammalian species. In the African wild dog, no distinct variance in neuronal density was observed, although the IOD appears to be slightly more myelin dense than the IOPr and IOM (Figure 16a,b). All neurons in these three nuclei appeared to be immunopositive for calbindin and calretinin, with a similar intensity of neuropil immunostaining observed in all nuclei, except for calretinin in the IOD which evinced a slightly paler calretinin neuropil-immunostaining (Figure 16c,d). A high proportion of the neurons were immunopositive for neurofilament H (Figure 16e), while an intense vesicular glutamate transporter 2-immunostaining of many neuronal structures was observed in all three nuclei (Figure 16f).

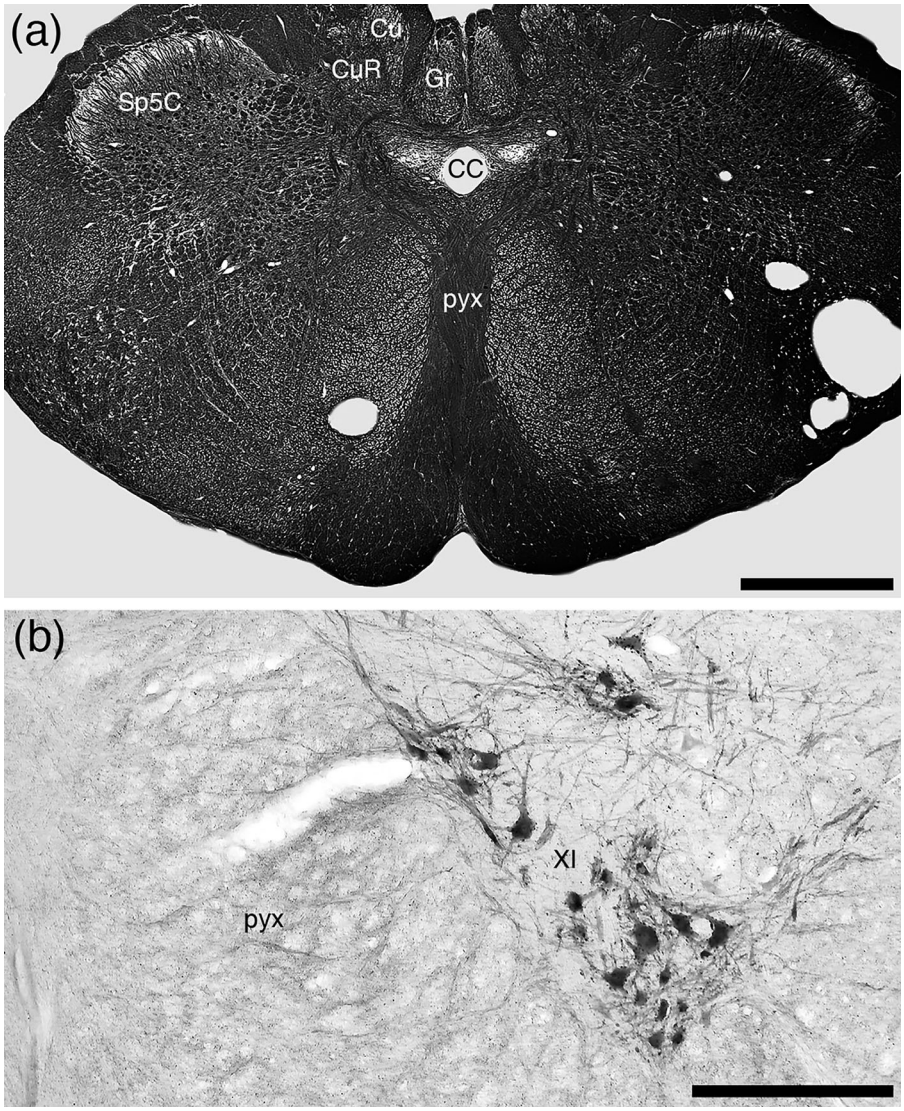

FIGURE 17 | Photomicrographs of coronal sections stained for (a) myelin, through the decussation of the pyramidal tract (pyx), and (b) choline acetyltransferase (ChAT) showing the accessory nerve nucleus (XI), at the spinomedullary junction in the African wild dog. CC—central canal; Cu—cuneate nucleus; CuR—rotundus part of the cuneate nucleus; Gr—gracile nucleus; Sp5C—caudal part of the spinal trigeminal nucleus. In both images, dorsal is to the top, and in image (b) the midline is to the left. Scale bar in (a) = 2 mm. Scale bar in (b) = 500 μm.

3.8 | Cranial Nerve Motor Nuclei and the Ventral Cervical Spinal Cord

Cranial nerve motor nuclei were observed throughout the brainstem and were found in positions typically observed in mammals; thus, we do not describe their location in detail. All neurons comprising these cranial nerve motor nuclei were found to be choline acetyltransferase-immunopositive (Figures 17b and 18–20). Located within the ventromedial periaqueductal gray matter, we observed the distinct oculomotor nucleus (III), with the trochlear nucleus (IV) located in the medioventrally adjacent midbrain tegmentum. The abducens nucleus (VI) was nestled within the genu of the facial nerve in the pons. These three nuclei that are responsible for eye movement showed no distinct augmentation when broadly compared to other mammals.

Within the rostral portion of the pontine tegmentum, the distinct motor trigeminal nucleus (Vmot) and the motor branch of the trigeminal nerve were readily observed with immunostaining for neuronal nuclear marker, choline acetyltransferase, and neurofilament H (Figure 18). In the ventrolateral aspect of the caudal pontine tegmentum, the facial nerve nucleus (VII) was observed. The VII nucleus was readily divisible into a smaller dorsal (VIId) and a substantially larger ventral (VIIv) part. While there appears to be slightly larger neurons in the lateral aspect of VIIv, we did not subdivide the VIIv as sometimes done in other mammals, although it is likely that a distinct musculotopy is present in this nucleus. In addition, choline acetyltransferase-immunopositive neurons representing the preganglionic motor neurons of the superior salivatory nucleus (pVII) were observed dorsolateral to the VIId (Figure 19).

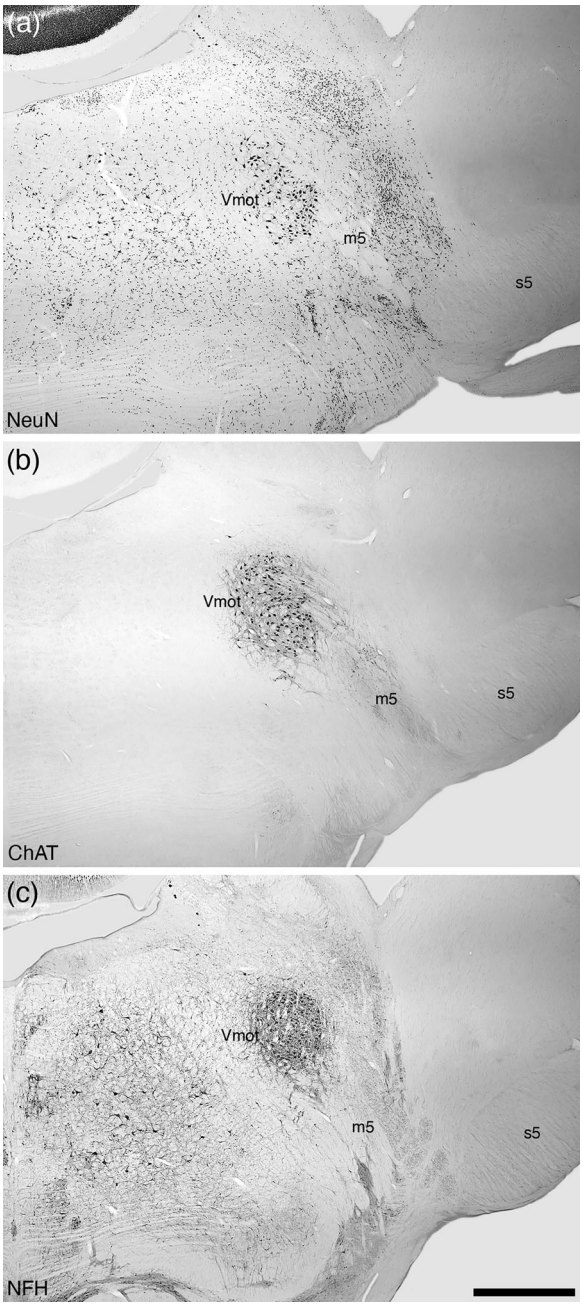

FIGURE 18 | Photomicrographs of coronal sections through the pons of the African wild dog stained with (a) neuronal nuclear marker (NeuN), (b) choline acetyltransferase (ChAT), and (c) neurofilament H (NFH). The motor trigeminal nucleus (Vmot) forms a distinct nucleus composed of large motoneurons in the lateral aspect of the pontine tegmentum. The motor (m5) and sensory (s5) roots of the trigeminal nerve are found ventrolateral to the Vmot. In all images, medial is to the left and dorsal to the top. Scale bar in (c) = 2 mm and applies to all.

In the medulla oblongata, we noted the presence of the nucleus ambiguus, the dorsal motor nucleus of the vagus nerve (X), and the hypoglossal nucleus (XII) (Figures 20 and 21). The nucleus ambiguus was composed of a loosely aggregated, radially oriented, column of choline acetyltransferase-immunopositive neurons in the ventrolateral aspect of the medullary tegmentum, extending from the caudal pole of VII through to the caudal portions of the medulla oblongata (Figure 20). The X formed a distinct dense cluster of relatively smaller neurons in the dorsal aspect of the caudal medulla, surrounded by the nuclear complex of the tractus solitarius (Figures 20 and 21). Located medioventrally adjacent to the X, the distinct XII was identified. Within the XII, there appeared to be three parts, the medial part (XIIm) composed of relatively smaller neurons, and the dorsolateral (XIIdl) and ventrolateral (XIIvl) parts composed of relatively larger neurons but distinguished by a soma-sparse lamella (Figures 20 and 21). With both choline acetyltransferase- and neurofilament H-immunostaining, a distinct, dorsally arched, fascicle of dendrites (known as protoplasmic commissural dendrites, see Section 4.2) was observed traversing the midline between the left and right XIIm's (Figures 20 and 21), although the immunoreactive staining for choline acetyltransferase was less intense than that observed for neurofilament H (Figure 20 insets e,f). This distinct midline traversing dendritic fascicle was apparent in the rostral 2 mm of XIIm (Figures 20 and 21). At the transition between the medulla oblongata and the spinal cord, a cluster of larger, cholinergic, motoneurons formed the accessory nerve nucleus (XI). The neurons forming the XI were located at the same level as the decussation of the pyramidal tract (Figures 17b and 21) and were the most rostral portion of a column of larger motor neurons that continued into the spinal cord. Within the ventral horn of the cervical spinal cord, we could readily identify laminae 7, 8, and 9 of the spinal grey matter (7Sp, 8Sp, 9Sp) (Figure 22). At the level of the cervical spinal cord examined, the 9Sp was parcellated into three distinct aggregations, two of these on the ventromedial aspect with one on the ventrolateral aspect of the ventral horn (Figure 22).

4 | Discussion

In this study, we have provided a qualitative systems-level analysis of the motor system in the brain of the African wild dog. This study builds on our analyses of the sensory systems in the African wild dog brain (Chengetanai et al. 2020b; Chengetanai et al. 2020d; Chengetanai et al. 2025), with the aim of determining whether any specializations related to the sociality of the African wild dog can be observed. We conclude for the motor system of the African wild dog, with one specific exception, that at the systems-level no overt specializations of the brain can be observed, particularly in comparison to the domestic dog (e.g., Singer 1962; Dattam et al. 2012). The one exception noted, that may be related to the sociality of the African wild dog, was the presence of a distinct fascicle of protoplasmic commissural dendrites in the rostral portion of the hypoglossal nucleus.

4.1 | Comparison of the Motor System of the African Wild Dog

In the African wild dog, we were able to delineate three distinct motor cortical areas, the primary motor cortex (M1, or Brodmann area 4), the premotor cortical area (PreM, or Brodmann area 6), and the SMA. Electrostimulation mapping studies of the motor cortex of the dog have revealed the presence of M1 and PreM (Woolsey 1933; W. K. Smith 1935; Górska 1974), although it appears the mesial wall of the hemisphere, where we identify the SMA of the African wild dog, has not been examined with this technique. All three motor cortical areas identified anatomically

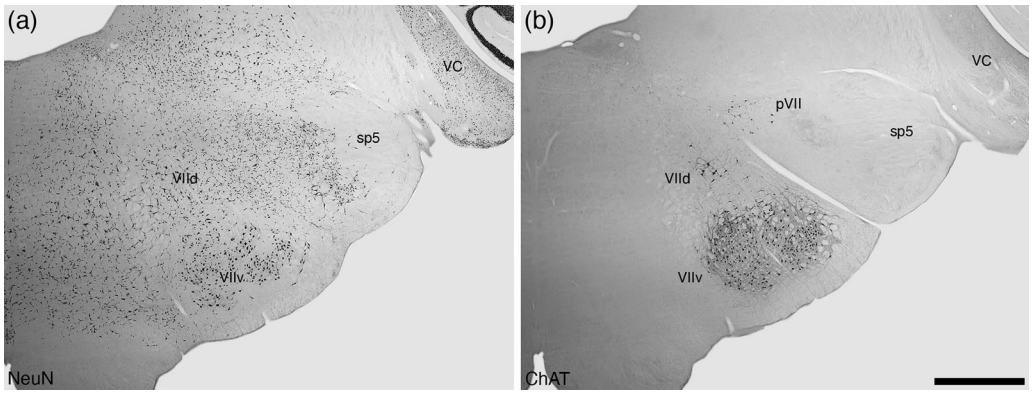

FIGURE 19 | Photomicrographs of coronal sections through the facial nerve nucleus of the African wild dog stained with (a) neuronal nuclear marker (NeuN), and (b) choline acetyltransferase (ChAT). Three components of the facial nerve nucleus were identified, the largest being the ventral division of the facial nerve nucleus (VIIv), as well as the dorsal division of the facial nerve nucleus (VIId), and the preganglionic motor neurons of the superior salivatory nucleus or facial nerve (pVII). In both images, medial is to the left and dorsal to the top. Scale bar in (b) = 2 mm and applies to both images. sp5—spinal trigeminal tract; VC—ventral cochlear nucleus.

in the African wild dog have been identified experimentally in the domestic cat (Nieoullon and Rispal-Padel 1976; Ghosh 1997). It is possible that these three cortical areas represent the homologous complement of motor cortical areas found in carnivores (e.g., Manger 2005), although further studies are needed to confirm this possibility.

Regarding the neurochemical aspects of the motor cortex of the African wild dog, we can make direct comparisons to that described M1 of the domestic dog (Hof et al. 1996), as we investigated the homologous area using four of the same antibodies (from the same manufacturers) in this study as used previously, these being those for neurofilament H (NFH), parvalbumin, calbindin, and calretinin. In the domestic dog, Hof et al. (1996) report that the NFH antibody labeled both soma and dendrites in layers 3 and 5, with the number structures labeled being higher in layer 5. We find the same pattern of staining of NFH in M1 of the African wild dog. In the African wild dog, parvalbumin immunostaining revealing soma and other structures was most intense in layers 3 and 5, with less intense staining in layers 2 and 6. This is precisely the same pattern reported for the domestic dog (Hof et al. 1996). In the domestic dog, calbindin-immunopositive soma and other structures were dense in layers 2 and 3, and while present in layers 5 and 6, were less dense (Hof et al. 1996), which is the same pattern as observed in the current study of the African wild dog M1. Calretinin immunostaining in M1 of the African wild dog revealed soma and other structures having their highest density in layer 2, with substantially lower densities of immunolabeled structures in layers 3, 5, and 6. Again, the same laminar pattern was observed in the domestic dog (Hof et al. 1996). We can conclude that the neurochemistry of M1 in the African wild dog and domestic dog is very similar. This indicates that the way neural information leading to motor commands is processed is likely to be very similar between the two species. This contrasts with our comparison of the primary somatosensory cortex of the African wild dog and domestic dog where while similar neurochemical laminar patterns were observed, variances in the expression of calbindin and neurofilament H were noted (Chengetanai et al. 2025).

The remainder of the motor system, apart from the one exception (see Section 4.2), also appears to be very similar to that observed in the domestic dog (e.g., Singer 1962; Dattam et al. 2012), and more broadly across mammals. For example, the structures revealed with parvalbumin, calbindin, and calretinin immunostaining in the cerebellar cortex of the African wild dog are precisely the same as observed in a range of other carnivore species (Bhagwandin et al. 2024). Given the extent of similarity, both in terms of the structures observed, their relative size as judged qualitatively, and the neurochemical similarity (e.g., for M1 and cerebellar cortex), it is fair to conclude that, with one exception, there are no overt changes to the motor system in the African wild dog that would appear to support the highly social life-history of this species (Van den Berghe et al. 2019; Creel and Creel 2002; Walker et al. 2017).

4.2 | A Potential Specialization in the Motor System of the African Wild Dog

The one clear variance noted in this study of the African wild dog motor system when compared to other species is the presence of a distinct fascicle of dendrites at the rostral end of the hypoglossal nucleus that cross the midline to terminate in the homologous nucleus. This midline-traversing dendritic fascicle, visualized with both choline acetyltransferase and neurofilament H immunostaining (Figure 20), although the staining intensity was weaker for choline acetyltransferase than neurofilament H, emerges from the soma of the motor neurons of the medial division of the hypoglossal nucleus (XIIm). A review of the hypoglossal system across vertebrates states that for mammals (Barnard 1940, 501): “At rostral levels of the nucleus there are strong commissural connections between the two hypoglossal nuclei,” but no further details are provided. The application of the term “commissural” to this midline-traversing hypoglossal dendritic fascicle in the African wild dog (or other species where it may be present, Barnard 1940) may not be entirely appropriate, as the term “commissure” typically refers to axon fascicles that cross the midline to terminate in contralateral homologous structures

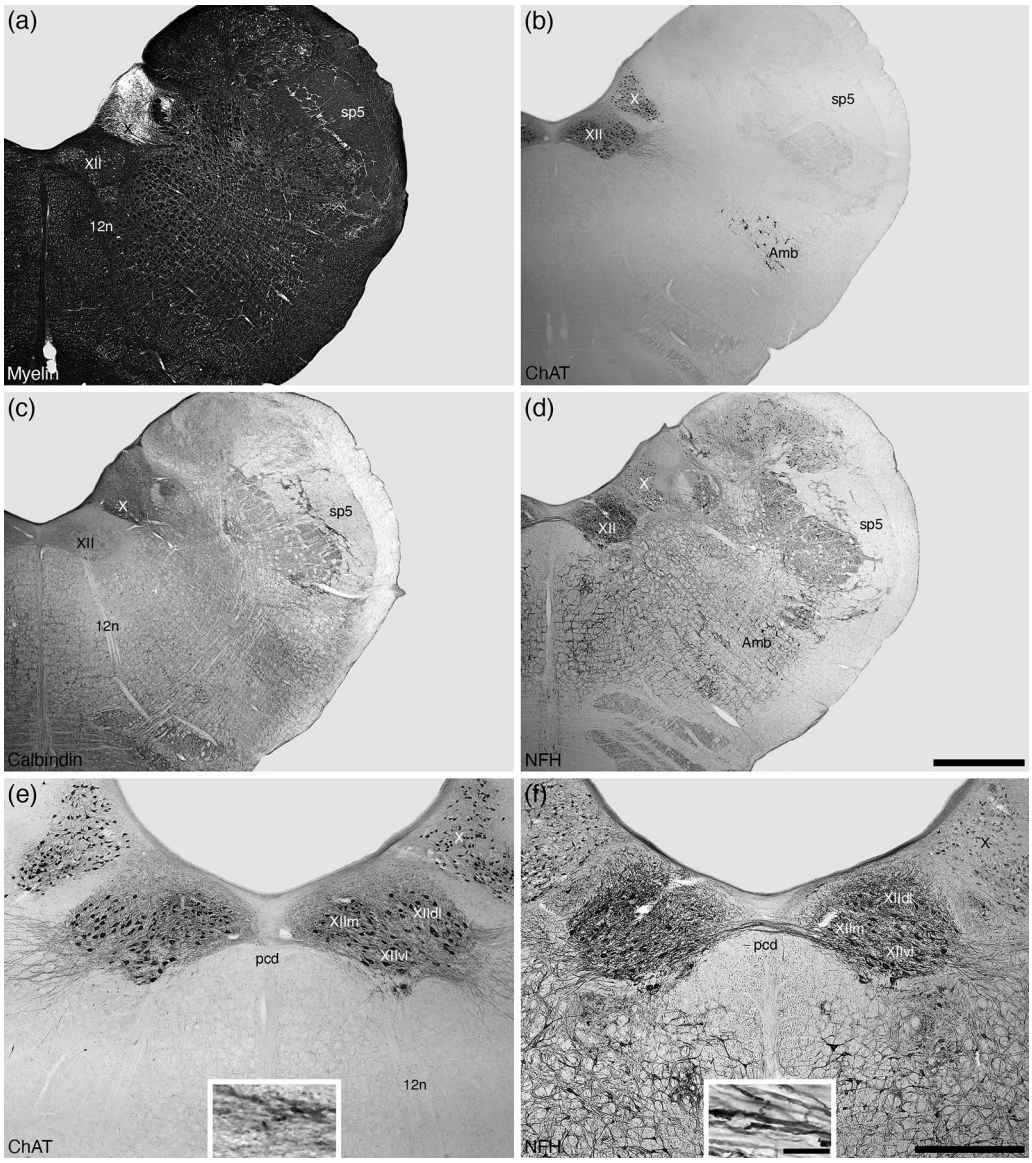

FIGURE 20 | Photomicrographs of adjacent coronal sections through the caudal medulla of the African wild dog stained with (a) myelin, (b, e) choline acetyltransferase (ChAT), (c) calbindin, and (d, f) neurofilament H (NFH). The dorsal motor vagus (X), hypoglossal (XII), and ambiguus (N.Amb), cranial nerve nuclei are located in positions similar to that observed in other species. Note the presence of three subdivisions within the XII, the dorsolateral (XIIdl), medial (XIIm), ventrolateral (XIIvl) parts, as well as the fascicle of protoplasmic commissural dendrites (pcd) between the bilateral XIIm parts of the XII nuclei (e, f), with dendrites also extending ventrolaterally from the XIIdl and XIIvl parts into the dorsolateral caudal medullary tegmentum (e, f). The high magnificent insets in (e) and (f) show the fascicle of protoplasmic commissural dendrites stained for ChAT (e) and NFH (f). In images (a–d), medial is to the left and dorsal to the top. In images (e) and (f), the midline is at the middle of the image and dorsal to the top. Scale bar in (d) = 2 mm and applies to (a–d). Scale bar in (f) = 1 mm and applies to (e) and (f). Scale bar in inset (f) = 25 μm and applies to insets (e) and (f). 12n—hypoglossal nerve.

(e.g., Graf 2011; Suárez 2017), rather than dendritic fascicles crossing the midline.

Hypoglossal motor neurons with dendrites that traverse the midline were, to our knowledge, first reported using Golgi-stained sections of the brain of a 4-day-old mouse by Ramón y Cajal (1909, 707, his fig. 291), referring to these dendrites as transverse filaments. Apart from the generalized statement of Barnard (1940), the only other reports in the literature of hypoglossal-hypoglossal connectivity that we could find were the studies of adult macaque and squirrel monkeys (Cooper 1981a) and rat (Cooper 1981b; Wan et al. 1982). Wan et al. (1982) injected tract tracers into the tongue of adult albino rats, revealing what they term hypoglossal nucleus "commissural dendrites" (see their fig. 1), but they also mention "protoplasmic commissural dendrites," and the "protoplasmic commissure of Van Gehuchten" (but provide no traceable reference to Van Gehuchten's work). Thus, to avoid potential confusion with traditionally defined commissures composed primarily of myelinated axons (e.g., Graf 2011; Suárez 2017), we refer to the midline traversing dendrites emanating from the respective left and right XIIm in the African wild dog as a fascicle of protoplasmic commissural dendrites.

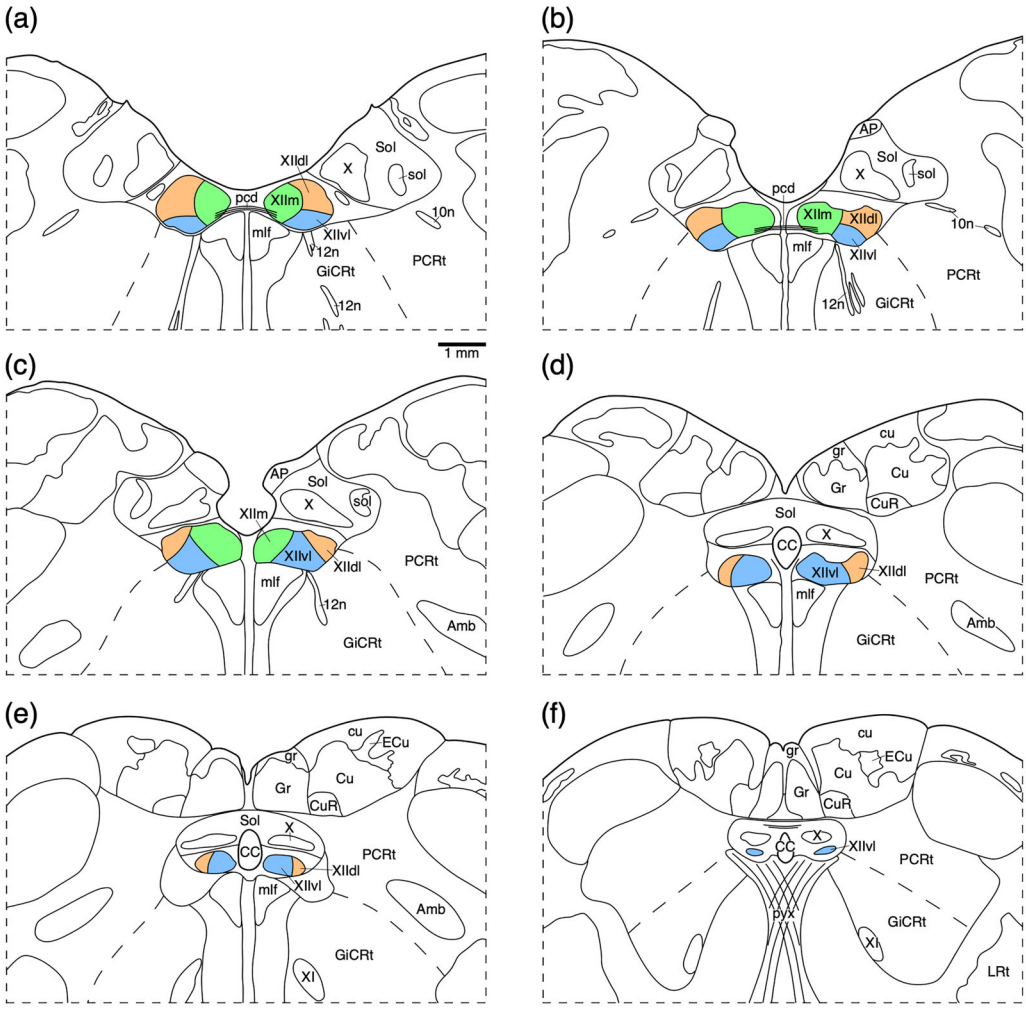

FIGURE 21 | Diagrammatic reconstructions of coronal sections through the African wild dog brain delineating the hypoglossal nucleus (XII) and adjacent structures. The most rostral section drawn is represented in (a), while the most caudal section is represented in (f). In all diagrams, dorsal is to the top, with each diagram being ~1000 μm apart. The XII nucleus of the African wild dog can be parcellated into three subnuclei, the medial (XIIm), ventrolateral (XIIvl), and dorsolateral (XIIdl), based on architectural criteria, such as the soma being smaller in the XIIm, and a distinct gap between the XIIvl and XIIdl. A distinct fascicle of protoplasmic commissural dendrites (pcd) is observed between the left and right XIIm subnuclei in the rostral portion of this nucleus. The various subdivisions of the hypoglossal nucleus are represented with differing colors. See the list for abbreviations.

The images provided by Cajal (1909), Cooper (1981a, 1981b), and Wan et al. (1982) show that in the mouse, rat, squirrel monkey, and macaque monkey, there is not a distinct fascicle of protoplasmic commissural dendrites connecting two clearly separated hypoglossal nuclei as we see in the African wild dog (Figure 20). Rather, these protoplasmic commissural dendrites are broadly distributed across the dorsoventral extent of the medially adjacent borders of the hypoglossal nucleus. Thus, our observation of a distinct fascicle of protoplasmic commissural dendrites in the African wild dog appears to be a novel observation, distinguishing the African wild dog from the studies of similar hypoglossal protoplasmic commissural dendrites in rodents and primates (Cajal 1909; Cooper 1981a, 1981b; Wan et al. 1982). Possibly, the genesis of this fascicle of protoplasmic commissural dendrites in the African wild dog may be the result of the fact that the hypoglossal nuclei are separated by over 500 μm, whereas in the rodents and primate studied, the medial borders of the hypoglossal nuclei are virtually adjacent. The increased mediolateral distance between the XIIm in the African wild dog may necessitate the formation of a distinct fascicle of protoplasmic commissural dendrites, rather than the simple projection of dendrites across the midline with no compartmentalized organization. It is possible that the protoplasmic commissural dendrites of the XIIm are also present in other canids and even other non-carnivore species, making this an interesting feature to investigate across mammals.

Functionally, Wan et al. (1982) propose that these protoplasmic commissural dendrites are likely to receive additional input, rather than just those projecting to the hypoglossal nucleus from which they emerge. While the corticobulbar projection to the hypoglossal nucleus is bilateral (Morecraft et al. 2014), it is predominantly contralateral. Thus, the protoplasmic commissural dendrites may provide an additional bilateral input, or modulation, of the hypoglossal motor neurons for control of the tongue. In the domestic dog, the medial division of the hypoglossal nucleus projects to the genioglossus muscle (Mu and Sanders 1999), which is divided into horizontal and oblique compartments that are involved in protrusion and depression of the

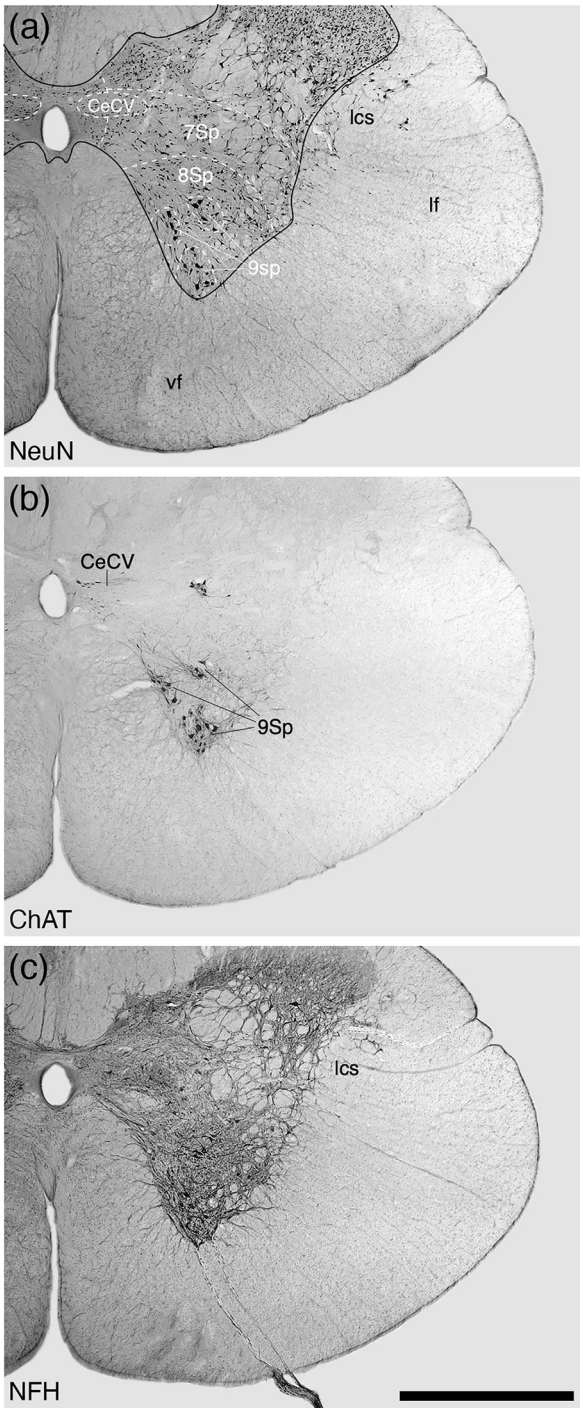

FIGURE 22 | Photomicrographs of adjacent coronal sections through the upper cervical spinal cord of the African wild dog stained with (a) neuronal nuclear marker (NeuN), (b) choline acetyltransferase (ChAT), and (c) neurofilament H (NFH). At this level of the spinal cord, we could identify, in the ventral horn, laminae 7 (7Sp), 8 (8Sp), and 9 (9Sp) of Rexed. 9Sp consisted of three distinct clusters of ChAT immunopositive neurons, possibly corresponding to flexor/extensor groupings. ChAT immunopositive neurons were also observed in the central cervical nucleus (CeCV), and slightly lateral to this nucleus in the upper portion of 7Sp. The fibers forming the lateral cortical spinal tract (lcs) are seen in the dorsal aspect of the lateral funiculus (lf) as well as passing through 7Sp and laminae 5. In all images, medial is to the left and dorsal to the top. Scale bar in (c) = 2 mm and applies to all. vf—ventral funiculus.

tongue, respectively. These horizontal and oblique compartments play a role in respiration and fine motor control of the tongue, respectively (Mu and Sanders 2000). As with other mammals, the hypoglossal nucleus of the dog receives corticobulbar input (Barnard 1940). Thus, we can make the reasonable assumption that the tongue of the African wild dog can be controlled through the corticobulbar pathway originating from the motor cortex. This means that the control of respiration and fine motor movement of the tongue in the African wild dog may be under more extensive bilateral modulation of XIIm neurons due to the presence of the distinct fascicle of protoplasmic commissural dendrites. Precisely how this possibly augmented bilateral modulation works remains to be determined.

The tongue of the African wild dog, in addition to normal functions associated with the tongue such as respiration and swallowing, is important in many social behaviors, including biting, licking, and vocalizations (Walker et al. 2017; Van den Berghe et al. 2019). In humans, the genioglossus muscle plays an important role in speech articulation and respiration (Mu and Sanders 2000). Given that the African wild dog is a highly vocal species (Walker et al. 2017; Robbins 2000; Robbins and McCreery 2003), it may be speculated that the fascicle of hypoglossal protoplasmic commissural dendrites may be involved in more precise control of the tongue during vocalization and thus improved articulation, thereby improving social behaviors mediated by vocalizations. It would be of interest to examine the structure of the rostral hypoglossal nucleus, especially the potential appearance and organization of protoplasmic commissural dendrites in other canid species such as the domestic dog, wolves, and other related carnivores such as bears and seals.

This line of reasoning leads to a potentially very interesting, but speculative, possibility. In humans, vocalizations (language) are clearly lateralized, with semantic and social aspects of language processed in different hemispheres (e.g., Rajimehr et al. 2022). Lateralization of vocalizations in other vertebrates is well established, although not extensively studied (Ocklenburg et al. 2013), with recent studies in domestic dogs providing evidence for lateralization of affect-laden human vocalizations (Gábor et al. 2020; Cuaya et al. 2022; Gergely et al. 2023). If, speculatively, the production of vocalizations by the African wild dog is lateralized, it may be that one cerebral hemisphere is involved in the semantic aspects of vocal production, while the other hemisphere contributes to the affective, social-context, aspects of vocalizations. The distinct fascicle of protoplasmic commissural dendrites observed in the African wild dog may potentially augment the melding of social context into the production of vocalizations, making their vocalizations far more nuanced than just the simple production of standardized vocalizations. Such a potential semantic/social merging in the hypoglossal nucleus, potentially augmented by the distinct fascicle of protoplasmic commissural dendrites if present in domestic dogs, might provide an elegant model to study the early appearance of vocal lateralization in mammals (Ocklenburg et al. 2013), indicating that the lateralization of semantic/social aspects of human language may be the result of a much earlier evolutionary feature of the brain than currently understood.

Author Contributions

P.R.M. and M.A.S. conceptualized the study. M.F.B. and T.H. obtained the brains. S.C., A.B., M.A.S., and P.R.M. performed the staining and analysis. S.C., P.R.H., M.A.S., and P.R.M. wrote the manuscript, and the remaining authors contributed to the editing and improvement of the early drafts of the manuscript. All authors had full access to all data in the study and take responsibility for the integrity of the data and the accuracy of the data analysis.

Acknowledgments

The authors have nothing to report.

Conflicts of Interest

Prof. Patrick Hof is an Editorial Board member of *The Journal of Comparative Neurology* and a co-author of this article. To minimize bias, he was excluded from all editorial decision-making related to the acceptance of this article for publication. The other authors declare no conflicts of interest.

Data Availability Statement

Data have not been shared due to this study being based on histological sections.

References

Barnard, J. W. 1940. "The Hypoglossal Complex of Vertebrates." *Journal of Comparative Neurology* 72: 489–524. https://doi.org/10.1002/cne.900720304.

Bertelsen, M. F. 2018. "Issues Surrounding Surplus Animals in zoos." In *Fowler's Zoo and Wild Animal Medicine, Current Therapy*, edited by R. E. Miller, N. Lamberski, and P. Calle, Vol. 9: 134–137. Elsevier.

Bhagwandin, A., C. C. Sherwood, P. R. Hof, et al. 2024. "Parvalbumin, Calbindin, and Calretinin Immunostaining of 10 Neural Structures Within the Cerebellar Cortex of 143 Mammal Species." *Frontiers in Mammal Science* 3: 1355791. https://doi.org/10.3389/fmamm.2024.1355791.

Buxton, D. F., and D. C. Goodman. 1967. "Motor Function and the Corticospinal Tracts in the Dog and Racoon." *Journal of Comparative Neurology* 129: 341–360. https://doi.org/10.1002/cne.901290405.

Celio, M. R. 1990. "Calbindin D-28k and Parvalbumin in the Rat Nervous System." *Neuroscience* 35: 375–475. https://doi.org/10.1016/0306-4522(90)90091-h.

Chengetanai, S., J. Tenley, M. F. Bertelsen, et al. 2020a. "The Brain of the African Wild Dog. I. Anatomy, Architecture, and Volumetrics." *Journal of Comparative Neurology* 528: 3245–3261. https://doi.org/10.1002/cne.24999.

Chengetanai, S., A. Bhagwandin, M. F. Bertelsen, et al. 2020b. "The Brain of the African Wild Dog. II. The Olfactory System." *Journal of Comparative Neurology* 528: 3285–3304. https://doi.org/10.1002/cne.25007.

Chengetanai, S., A. Bhagwandin, M. F. Bertelsen, et al. 2020c. "The Brain of the African Wild Dog. III. The Auditory System." *Journal of Comparative Neurology* 528: 3229–3244. https://doi.org/10.1002/cne.24989.

Chengetanai, S., A. Bhagwandin, M. F. Bertelsen, et al. 2020d. "The Brain of the African Wild Dog. IV. The Visual System." *Journal of Comparative Neurology* 528: 3262–3284. https://doi.org/10.1002/cne.25000.

Chengetanai, S., A. Bhagwandin, M. F. Bertelsen, et al. 2025. "The Brain of the African Wild Dog. V. The Somatosensory System and Vestibular Nuclear Complex." *Journal of Comparative Neurology*.

Cooper, M. H. 1981a. "The Hypoglossal Nucleus of the Primate: A Golgi Study." *Neuroscience Letters* 21: 249–254. https://doi.org/10.1016/0304-3940(81)90212-3.

Cooper, M. H. 1981b. "Neurons of the Hypoglossal Nucleus of the Rat." *Otolaryngology—Head and Neck Surgery* 89: 10–15. https://doi.org/10.1177/019459988108900103.

Creel, S., and N. M. Creel. 2002. *The African Wild Dog. Behavior, Ecology, and Conservation*. Princeton University Press.

Cuaya, L. V., R. Hernández-Pérez, M. Boros, A. Deme, and A. Andics. 2022. "Speech Naturalness Detection and Language Representation in the Dog Brain." *NeuroImage* 248: 118811. https://doi.org/10.1016/j.neuroimage.2021.118811.

Dattam, R., J. Lee, J. Duda, et al. 2012. "A Digital Atlas of the Dog Brain." *PLoS ONE* 7: e52140. https://doi.org/10.1371/journal.pone.0052140.

Floresco, S. B. 2015. "The Nucleus Accumbens: An Interface Between Cognition, Emotion, and Action." *Annual Review of Psychology* 66: 25–52. https://doi.org/10.1146/annurev-psych-010213-115159.

Foster, M., S. Dwibhashyam, D. Patel, et al. 2024. "Comparative Anatomy of the Caudate Nucleus in Canids and Felids: Associations With Brain Size, Curvature, Cross-Sectional Properties, and Behavioral Ecology." *Journal of Comparative Neurology* 532: e25618. https://doi.org/10.1002/cne.25618.

Gábor, A., M. Gácsi, D. Szabó, Á. Miklósi, E. Kubinyi, and A. Andics. 2020. "Multilevel fMRI Adaptation for Spoken Word Processing in the Awake Dog Brain." *Scientific Reports* 10: 11968. https://doi.org/10.1038/s41598-020-68821-6.

Gallyas, F. 1979. "Silver Staining of Myelin by Means of Physical Development." *Neurological Research* 1: 203–209. https://doi.org/10.1080/01616412.1979.11739553.

Gergely, A., A. Gábor, M. Gácsi, et al. 2023. "Dog Brains Are Sensitive to Infant- and Dog-Directed Prosody." *Communications Biology* 6: 859. https://doi.org/10.1038/s42003-023-05217-y.

Ghosh, S. 1997. "Identification of Motor Areas of the Cat Cerebral Cortex Based on Studies of Cortical Stimulation and Corticospinal Connections." *Journal of Comparative Neurology* 380: 191–214. https://doi.org/10.1002/(sici)1096-9861(19970407)380::2⟨191::aid-cne4⟩3.0.co;2-z.

Górska, T. 1974. "Functional Organization of Cortical Motor Areas in Adult Dogs and Puppies." *Acta Neurobiologiae Experimentalis (Warsaw)* 34: 171–203.

Graf, M. R. 2011. "Commissures, Cerebral." In *Encyclopedia of Clinical Neuropsychology*, edited by J.S. Kreutzer, J. DeLuca, and B. Caplan, 650. Springer. https://doi.org/10.1007/978-0-387-79948-3_307.

Griffin, G. D., S. L. Ferri-Kolwicz, B. A. S. Reyes, E. J. van Bockstaele, and L. M. Flanagan-Cato. 2010. "Ovarian Hormone-Induced Reorganization of Oxytocin-Labeled Dendrites and Synapses Lateral to the Hypothalamic Ventromedial Nucleus in Female Rats." *Journal of Comparative Neurology* 518: 4531–4545. https://doi.org/10.1002/cne.22470.

Hof, P. R., Y. E. Bogaert, R. E. Rosenthal, and G. Fiskum. 1996. "Distribution of Neuronal Populations Containing Neurofilament Protein and Calcium-Binding Proteins in the Canine Cortex: Regional Analysis and Cell Typology." *Journal of Chemical Neuroanatomy* 11: 81–98. https://doi.org/10.1016/0891-0618(96)00126-3.

Jones, E. G. 2007. *The Thalamus*. Cambridge University Press.

Kaiser, A., O. Alexandrova, and B. Grothe. 2011. "Urocortin-Expressing Olivocochlear Neurons Exhibit Tonotopic and Developmental Changes in the Auditory Brainstem and in the Innervation of the Cochlea." *Journal of Comparative Neurology* 519: 2758–2778. https://doi.org/10.1002/cne.22650.

Laux, A., F. Delalande, J. Mouheiche, et al. 2012. "Localization of Endogenous Morphine-Like Compounds in the Mouse Spinal Cord." *Journal of Comparative Neurology* 520: 1547–1561. https://doi/org/10.1002/cne.22811.

Manger, P. R. 2005. "Establishing Order at the System Level in Mammalian Brain Evolution." *Brain Research Bulletin* 66: 282–289. https://doi.org/10.1016/j.brainresbull.2005.05.002.

Meredith, G. E., R. Agolia, M. P. M. Arts, H. J. Groenewegen, and D. S. Zahm. 1992. "Morphological Differences Between Projection Neurons of the Core and Shell in the Nucleus Accumbens of the Rat." *Neuroscience* 50: 149–162. https://doi.org/10.1016/0306-4522(92)90389-J.

Møller, A. R. 2006. "Anatomy and Physiology of Motor Systems." In *Intraoperative Neurophysiological Monitoring*, edited by A. R. Møller, 157–178. Humana Press. https://doi.org/10.1007/978-1-59745-018-8_9.

Morecraft, R. J., K. S. Stilwell-Morecraft, K. M. Solon-Cline, J. Ge, and W. G. Darling. 2014. "Cortical Innervation of the Hypoglossal Nucleus in the Non-Human Primate (*Macaca mulatta*)." *Journal of Comparative Neurology* 522: 3456–3484. https://doi.org/10.1002/cne.23614.

Mu, L., and I. Sanders. 1999. "Neuromuscular Organization of the Canine Tongue." *Anatomical Record* 256: 412–424. https://doi.org/10.1002/(SICI)1097-0185(19991201)256:4⟨412::AID-AR8⟩3.0.CO;2-5.

Mu, L., and I. Sanders. 2000. "Neuromuscular Specializations of the Pharyngeal Dilator Muscles: II. Compartmentalization of the Canine Genioglossus Muscle." *Anatomical Record* 260: 308–325. https://doi.org/10.1002/1097-0185(20001101)260:3⟨308::AID-AR70⟩3.0.CO;2-N.

Nieoullon, A., and L. Rispal-Padel. 1976. "Somatotopic Localization in Cat Motor Cortex." *Brain Research* 105: 405–422. https://doi.org/10.1016/0006-8993(76)90590-4.

Ngwenya, A., N. Patzke, P. R. Manger, and S. Herculano-Houzel. 2016. "Continued Growth of the Central Nervous System Without Mandatory Addition of Neurons in the Nile Crocodile (*Crocodylus niloticus*)." *Brain, Behavior and Evolution* 87: 19–38. https://doi.org/10.1159/000443201.

Ocklenburg, S., F. Ströckens, and O. Güntürkün. 2013. "Lateralisation of Conspecific Vocalisations in Non-Human Vertebrates." *Laterality* 18: 1–31. https://doi.org/10.1080/1357650X.2011.626561.

Partanen, J., and K. Achim. 2022. "Neurons Gating Behavior—Developmental, Molecular and Functional Features of Neurons in the Substantia Nigra Pars Reticulata." *Frontiers in Neuroscience* 16: 976209. https://doi.org/10.3389/fnins.2022.976209.

Paxinos, G., C. Watson, P. Carrive, M. T. K. Kirkcaldie, and K. Ashwell. 2009. "Chemoarchitectonic Atlas of the Rat Brain." Elsevier.

Piskuric, N. A., C. Vollmer, and C. A. Nurse. 2011. "Confocal Immunofluorescence Study of Rat Aortic Body Chemoreceptors and Associated Neurons *in Situ* and *in Vitro*." *Journal of Comparative Neurology* 519: 856–873. https://doi.org/10.1002/cne.22553.

Prevosto, V., and M. A. Sommer. 2013. "Cognitive Control of Movement *via* the Cerebellar-Recipient Thalamus." *Frontiers in Systems Neuroscience* 7: 56. https://doi.org/10.3389/fnsys.2013.00056.

Ramón y Cajal, S. 1909. *Histologie Du Système Nerveux De L'Homme et Des Vertébrés*. A. Maloine.

Rajimehr, R., A. Firoozi, H. Rafipoor, N. Abbasi, and J. Duncan. 2022. "Complementary Hemispheric Lateralization of Language and Social Processing in the Human Brain." *Cell Reports* 41: 111617. https://doi.org/10.1016/j.celrep.2022.111617.

Robbins, R. L. 2000. "Vocal Communication in Free-Ranging African Wild Dogs (*Lycaon pictus*)." *Behaviour* 137: 1271–1298.

Robbins, R. L., and E. K. McCreery. 2003. "African Wild Dog Pup Vocalizations With Special Reference to Morton's Model." *Behaviour* 140: 333–351.

Sakai, S. T., G. B. Stanton, and D. Tanaka Jr.. 1983. "The Ventral Lateral Thalamus Nucleus in the Dog: Cytoarchitecture, Acetylcholinesterase Histochemistry, and Cerebellar Afferents." *Brain Research* 271: 1–9. https://doi.org/10.1016/0006-8993(83)91359-8.

Schwaller, B., I. Durussel, D. Jermann, B. Herrmann, and J. A. Cox. 1997. "Comparison of the Ca^{2+}-Binding Properties of Human Recombinant Calretinin-22k and Calretinin." *Journal of Biological Chemistry* 272: 29633–29671.

Singer, M. 1962. *The Brain of the Dog in Section*. W.B. Saunders Company.

Smith, W. K. 1935. "The Extent and Structure of the Electrically Excitable Cerebral Cortex in the Frontal Lobe of the Dog." *Journal of Comparative Neurology* 62: 421–442. https://doi.org/10.1002/cne.900620209.

Smith, H. F., B. Adrian, R. Koshy, R. Alwiel, and A. Grossman. 2020. "Adaptations to Cursoriality and Digit Reduction in the Forelimb of the African Wild Dog (*Lycaon pictus*)." *PeerJ* 8: e9866. https://doi.org/10.7717/peer.9866.

Sternberger, L. A., and N. H. Sternberger. 1983. "Monoclonal Antibodies Distinguish Phosphorylated and Nonphosphorylated Forms of Neurofilaments *in Situ*." *Proceedings of the National Academy of Science USA* 80: 6126–6130. https://doi.org/10.1073/pnas.80.19.6126.

Suárez, R. 2017. "Evolution of Telencephalic Commissures: Conservation and Change of Developmental Systems in the Origin of Brain Wiring novelties." In *Evolution of Nervous Systems*, edited by J.H. Kaas, 2nd ed., Vol. 2, 205–223. Elsevier. https://doi.org/10.1016/B978-0-12-804042-3.00042-7.

Väätäjä, H., P. Majaranta, A. V. Cardó, et al. 2021. "The Interplay Between Affect, Dog's Physical Activity and Dog-Owner Relationship." *Frontiers in Veterinary Science* 8: 673407. https://doi.org/10.3389/fvets.2021.673407.

Van den Berghe, F., M. C. J. Paris, Z. Sarnyai, et al. 2019. "Dog Appeasing Pheromone Prevents the Androgen Surge and May Reduce Contact Dominance and Active Submission After Stressful Interventions in African Wild Dogs (*Lycaon pictus*)." *PLoS ONE* 14: e0212551. https://doi.org/10.1371/journal.pone.0212551.

Walker, R. H., A. J. King, J. W. McNutt, and N. R. Jordan. 2017. "Sneeze to Leave: African Wild Dogs (*Lycaon pictus*) Use Variable Quorum Thresholds Facilitated by Sneezes in Collective Decisions." *Proceedings of the Royal Society B: Biological Sciences* 284: 20170347. https://doi.org/10.1098/rspb.2017.0347.

Wan, X. S. T., J. Q. Trojanowski, J. O. Gonatas, and C. N. Liu. 1982. "Cytoarchitecture of the Extranuclear and Commissural Dendrites of Hypoglossal Nucleus Neurons as Revealed by Conjugates of Horseradish Peroxidase With Cholera Toxin." *Experimental Neurology* 78: 167–175. https://doi.org/10.1016/0014-4886(82)90198-4.

Wong, P., O. A. Gharbawie, L. E. Luethke, and J. H. Kaas. 2008. "Thalamic Connections of Architectonic Subdivisions of Temporal Cortex in Grey Squirrels (*Sciurus carolinensis*)." *Journal of Comparative Neurology* 510: 440–461. https://doi.org/10.1002/cne.21805.

Woolsey, C. N. 1933. "Postural Relations of the Frontal and Motor Cortex of the Dog." *Brain* 56: 353–370. https://doi.org/10.1093/brain/56.4.353.